C172

NATIONAL AERONAUTICS AND SPACE ADMINISTRATION

EXTERNAL INSULATION AS A MEANS OF IMPROVING CRYOGENIC STORAGE SYSTEM THERMAL PERFORMANCE

INTERNAL NOTE NO. MSC-EP-R-67-15

AUTHORS: Pat B. McLaughlan
Richard J. Boyer

RECEIVED AUG 1970 NASA STI FACILITY INPUT BRANCH

N70-34393

FACILITY FORM 602

(ACCESSION NUMBER) 68
(PAGES) TMX-64393
(NASA CR OR TMX OR AD NUMBER)

(THRU) 1
(CODE) 11
(CATEGORY)

Thermochemical Test Branch
Propulsion and Power Division

MANNED SPACECRAFT CENTER
HOUSTON, TEXAS

July 5, 1967

Reproduced by
NATIONAL TECHNICAL
INFORMATION SERVICE
Springfield, Va. 22151

THERMOCHEMICAL TEST AREA
PROPULSION AND POWER DIVISION
NASA - MANNED SPACECRAFT CENTER
HOUSTON, TEXAS

INTERNAL NOTE NO. MSC-EP-R-67-15

EXTERNAL INSULATION AS A MEANS OF IMPROVING CRYOGENIC STORAGE SYSTEM THERMAL PERFORMANCE

DOC. NO. MSC-EP-R-67-15 DATE 7-5-67

PREPARED BY:	Pat B. McLaughlan	Pat B. McLaughlan
	Richard J. Boyer	Richard J. Boyer
APPROVED BY:	(SECTION)	
APPROVED BY:	(BRANCH OFFICE) Allen H. Watkins	for Fredon J. Heath
APPROVED BY:	(DIVISION) Joseph G. Thibodaux, Jr.	Richard B. Ferguson for
APPROVED BY:		

NO. OF PAGES 35

DOC. NUMBER MSC-EP-R-67-15

REVISIONS

DATE	AUTHOR	APPROVALS				CHG. LETTER
		SECTION	BRANCH	DIVISION		

MSC FORM 360A (JAN 67)

TABLE OF CONTENTS

Section - Page

INTRODUCTION

The primary objective of the test program was to evaluate the effectiveness of external insulation as a means of improving the thermal performance of a cryogenic storage system (CSS). Evaporation rate tests, using liquid nitrogen as the test fluid, were the basis for defining thermal performance. The CSS exterior was wrapped with laminar insulation and the thermal performance (heat leak) of the system was evaluated as a function of insulation thickness and environmental temperature. All thermal performance tests using external insulation were conducted in a vacuum environment of 10^{-5} torr or better. Baseline thermal performance data were established prior to the application of the external insulation.

A secondary objective of the program was to investigate the structural integrity of the insulation. The externally insulated CSS was subjected to rapid external decompressions, similar to those expected during launch operations.

The test article was a Bendix "Phase-B" oxygen CSS, modified for this test by the installation of a vapor cooling line on the outer shell and revision of the mounting structure. The CSS was procured from the Pioneer-Central Division of the Bendix Corporation, Davenport, Iowa, under NASA contract number NAS 9-2978. The CSS was delivered to NASA-MSC on February 8, 1966, and was tested without external insulation from February 28 to April 14, 1966. The results of the original test program were reported in Internal Note number MSC-IN-67-EP-10.

The tests were conducted by the Thermochemical Test Branch for the Power Generation Branch of the Propulsion and Power Division. Thermal performance tests were conducted at the Space Chamber Test Facility, Building 351, and the launch decompression tests were conducted at the Auxiliary Propulsion Test Facility, Building 353. The test program was accomplished during the period from March 20 to June 26, 1967.

TEST ARTICLE DESCRIPTION

The supercritical oxygen cryogenic storage system was designed and manufactured by the Pioneer-Central Division of the Bendix Corporation. It is designated as the "Phase-B" oxygen system to indicate that fabrication was accomplished during the second phase of the development contract. Figure 1 is a representative cut-away illustration of the system.

The CSS consists of two shells; an outer shell and a spherical inner pressure vessel. The inner pressure vessel, formed by the Ardeform process, is constructed of type 301 stainless steel. Internal insulation consists of an evacuated annulus containing two silver-plated aluminum radiation shields that are supported by the fill and vent lines. The inside diameter of the vessel is 25 inches, which corresponds to a volume of 4.74 feet^3 and a maximum capacity of 239 pounds of nitrogen.

A cylindrical subassembly consisting of two 176-watt heaters, two electric motor-fan units, four copper-constantan thermocouples and a capacitance probe is contained in the inner vessel. These components were not operated during the external insulation test.

The outer surface of the inner vessel is silver plated. The vessel is supported by eight Kel-F cylindrical supports: four mounted on the fill line and four mounted on the vent line.

The outer shell of the CSS is constructed of type 304L stainless steel and has a diameter of 29 inches. Its inner surface is copper plated. Mounted on the outer shell are two small (0.2 liter/second) ion pumps. These ion pumps permit re-evacuation of the annulus in the event of vacuum degradation and also serve as a gage attachment to monitor the annular vacuum level.

The CSS was originally supported by means of a mounting carriage which was located externally to the inner vessel supports. For the external insulation test this mounting carriage was removed to facilitate insulation application. The revised CSS support system, the vapor cooling line for the outer shell, and the external insulation are discussed in the test procedure section.

TEST PROGRAM

The test program consists of the thermal performance and decompression test sequences shown in the following table.

Sequence	External Insulation	Vapor Cooling	Environment
Nitrogen Thermal Performance Test			
1	None	No	70° F, Ambient Pressure
2	None	No	70° F, Vacuum
3	None	Yes	70° F, Vacuum
4	50 layers	Yes	0° F, Vacuum
5	50 layers	Yes	70° F, Vacuum
6	50 layers	Yes	140° F, Vacuum
7	100 layers	Yes	0° F, Vacuum
8	100 layers	Yes	70° F, Vacuum
9	25 layers	No	70° F, Vacuum
10	25 layers	Yes	0° F, Vacuum
11	25 layers	Yes	70° F, Vacuum
12	25 layers	Yes	140° F, Vacuum
13	5 layers	Yes	70° F, Vacuum
Decompression Test			
1	100 layers		
2	25 layers		

TEST PROCEDURE

This section is divided into three discussions. The first concerns installation and wrapping operations, the second concerns the thermal performance test operations, and the third concerns the decompression test operations.

Installation and Wrapping Operations

Figure 2 illustrates the support fixture used in both phases of the test program. The object of this fixture was to isolate the CSS from major thermal conduction paths through the CSS mounting structure. The spherical outer shell was supported on four teflon cylinders equally spaced (to coincide with the internal support bumpers) on a support ring formed from 1-inch diameter stainless steel tubing. The support ring was suspended from a cubical frame by 1/16-inch diameter stainless steel cables. The external insulation was applied over the support ring. The fill and vent ports were 1/8-inch sch 40 stainless steel pipe and remained attached to the CSS during the test.

The CSS was modified by removing the support carriage and all other exterior components (pressure switches, relief valves, electrical connectors, and fill and vent valves). The removal of these exterior components resulted in a smooth CSS outer surface except for the ion pump, the fill and vent port penetrations, the vapor cooling line, and the support ring.

Vapor cooling capability was not included in the original design; it was added to the CSS outer shell for the external insulation test. The purpose of this feature was to reduce the outer shell temperature (exiting vent gas removes heat), thereby reducing the effective heat leak. The vapor cooling line originated at the CSS vent port and consisted of four equally spaced wraps of 1/8-inch outside diameter by 0.030-inch wall copper tubing bonded to the CSS with epoxy. The enamel finish on the CSS outer shell was removed along the path of the vapor cooling line to allow bonding to bare metal. Aluminum powder was added to the epoxy for improved heat transfer. Figure 3 illustrates the CSS prior to the application of the external insulation and also illustrates the vapor cooling line.

The insulation used throughout this test program was a 1/4-mil polyester film which had been aluminized and crinkled for use as a multilayer reflective insulation. The insulation is a product of the National Research Corporation and is designated as NRC-2.

NRC-2 insulation operates on the principle of multilayer radiation barriers; certain physical conditions are essential for its effective use. First, gaseous conduction must be essentially eliminated by establishing and maintaining interstitial pressure levels of less than 10^{-4} torr. Second, NRC-2 should be installed to minimize solid conduction paths through the multilayers and to prevent lateral gradient along the multilayers. Based on the manufacturer's information, performance optimization is usually achieved with 60 to 70 layers per inch. As the spaces between the layers must be maintained at a pressure less than

10^{-4} torr, the edges of the layers should be joined only as needed to keep the material in place. Venting must be provided.

A rigorous procedure was not maintained for the application of the external insulation. Each layer of laminar insulation was formed from a rectangular sheet. The sheet was not cut to a pattern prior to application around the CSS outer shell. Each sheet was initially wrapped around the CSS and then formed to the spherical exterior by appropriate cutting of excess material and taping of the loose ends of the insulation. The insulation was applied layer by layer rather than by cutting and fitting a blanket of several layers at once. The insulation width and length was sufficient to allow a minimum overlap of 2 inches at all joints. The external insulation was wrapped over the exterior of the CSS to cover the support ring and the ion pump protrusion. In the final configuration, the only insulation penetrations were the fill and vent lines, the support ring rods, and the temperature sensor instrumentation leads. The sheet of laminar insulation was cut to lie around the fill, vent, and support ring rod penetrations. These penetrations were wrapped with teflon tape to minimize thermal shorting to the insulation. The insulation was not tightly drawn around the CSS but was allowed to remain slack during the application of each layer, since excess tension tends to decrease the effectiveness of the insulation.

As each additional layer of insulation was applied, the wrap was started in a different place; therefore, each wrap was a unique pattern and overlapping joints fell in a different area for each layer.

Figures 4 and 5 illustrate the application of the external insulation. Figure 6 illustrates the completely insulated CSS in the test fixture.

Thermal Performance Testing

All thermal performance tests with external insulation were conducted in a 15-foot spherical thermal vacuum chamber at pressure levels of 10^{-5} torr or better.

The CSS was installed in the chamber, as shown in figure 7, and filled with liquid nitrogen from a facility supply dewar until liquid discharge was noted from the vent. Figure 8 illustrates the liquid transfer and gas flow schematic. The chamber was then closed off and evacuated at a rate less than 1 psi/minute. The CSS was then allowed to vent (external to the chamber) until a stable flow rate was attained under the desired operational conditions (that is, at varied environmental temperatures with and without vapor cooling and with varied thicknesses of external insulation). The CSS was filled only once at each insulation thickness, and the low evaporation rates permitted completion of several sequences without refilling. For example, sequences 9 through 12 were completed without refilling. Following each series of sequences at a fixed insulation thickness, the chamber was repressurized, the insulation removed, and the CSS completely rewrapped to another insulation thickness.

Throughout the thermal performance test, the following parameters were recorded by a digital data acquisition system: CSS pressure, CSS nitrogen evaporation rate, CSS outer shell temperature, intermediate temperatures through the external insulation, environmental temperature and pressure, and the support ring temperatures. The digital data acquisition system is illustrated in figure 9. Figure 10 is a schematic of the instrumentation and data acquisition setup. CSS pressure was measured by a strain gage pressure transducer, nitrogen evaporation rate was measured with both a thermal mass flowmeter and a wet test flowmeter, and outer shell and laminar insulation temperatures were indicated by platinum resistance temperature transducers (RTT).

The RTT patches were bonded to the outer shell with epoxy and attached to the laminar insulation with tape. The size of the instrumentation wiring to the RTT was minimized to reduce heat conduction, and the wiring was brought through the insulation at a point 12 inches or greater from the sensor location. The following table indicates the location of the RTT for each of the test sequences.

RTT LOCATION - SEQUENCE 1 THROUGH 13

CSS outer shell, near vent port
CSS outer shell, girth
CSS outer shell, near fixture support pad
CSS outer shell, near end of vapor cooling line

ADDITIONAL RTT LOCATION - SEQUENCE 4, 5, 6

External insulation, 12th layer - girth
External insulation, 24th layer - girth
External insulation, 36th layer - girth
Exterior of external insulation, 50th layer - near fill line
Exterior of external insulation, 50th layer - top
Exterior of external insulation, 50th layer - bottom

ADDITIONAL RTT LOCATION - SEQUENCE 7, 8

External insulation, 12th layer - girth
External insulation, 24th layer - girth
External insulation, 36th layer - girth
External insulation, 75th layer - girth
Exterior of external insulation, 100th layer - south girth
Exterior of external insulation, 100th layer - north girth

ADDITIONAL RTT LOCATION - SEQUENCE 9, 10, 11, 12

External insulation, 6th layer - girth
External insulation, 12th layer - girth
External insulation, 18th layer - girth
Exterior of external insulation, 25th layer - west girth
Exterior of external insulation, 25th layer - south girth
Exterior of external insulation, 25th layer - north girth

ADDITIONAL RTT LOCATION - SEQUENCE 13

External insulation, 2nd layer - girth
External insulation, 3rd layer - girth
External insulation, 4th layer - girth
Exterior of external insulation, 5th layer - west girth
Exterior of external insulation, 5th layer - south girth
Exterior of external insulation, 5th layer - north girth

The temperatures at the support ring were indicated by 12 copper-constantan thermocouples (T/C). Figure 11 is a schematic location of the support ring T/C and surface RTT. The atmospheric pressure was continuously monitored by a recording barometer for all tests except sequences 4, 5, and 6.

Decompression Testing

The decompression test operations were conducted in a 20-foot spherical altitude chamber at the Auxiliary Propulsion Test Facility. The chamber was evacuated by means of a steam ejector; the pumpdown rate was slightly less than the decompression profile expected during a Saturn V launch. The empty CSS was installed in the chamber. The only data acquired during this phase of testing were from three motion picture cameras and two pressure transducers, which correlated insulation behavior and pressure. Two test sequences were conducted at insulation thicknesses of 100 layers and 25 layers.

RESULTS AND DISCUSSION

Thermal Performance Tests

The thermal performance evaluation was based on 13 individual nitrogen evaporation rate tests. The tests were conducted on the CSS under the following conditions: with no external insulation and with 5, 25, 50, and 100 layers of external insulation; in both vapor-cooled and non-vapor-cooled operational modes; at atmospheric pressure and high-vacuum environments; and in temperature environments ranging from 0° to 140° F. All high-vacuum tests were at a vacuum of 10^{-5} torr or better.

Table I defines the test conditions and summarizes the test results. The results were derived from the following definitions and procedures:

a. The heat leak value for this report is defined as the product of the nitrogen evaporation rate (as measured by a flowmeter external to the CSS) and the latent heat of vaporization of the liquid nitrogen.

b. The absolute pressure of the CSS must remain constant throughout the final evaporation rate measurement period to ensure an equilibrium of thermodynamic properties.

c. Latent heat of vaporization is a function of CSS pressure.

d. The total test time indicates the total duration of the evaporation rate test.

e. The elapsed time (ET) for the evaporation rate average indicates the ET span over which the final evaporation rate was averaged (a 10-hour period at the completion of each sequence except sequence 1, 2, and 11 where the evaporation rate was averaged over a 5-hour period). The evaporation rate average period may not correspond to the end of the total test time (as in sequence 9) if an analysis of the atmospheric pressure indicated the evaporation rate fluctuations were due to barometric pressure changes. A period of relatively stable barometric pressure always corresponded to the final average. Figure 12 illustrates the effect of barometric pressure fluctuations on the evaporation rate. The total variation during the evaporation rate average period indicates the minimum and maximum of the hourly flowmeter readings.

f. Average outer shell temperature was established from the four peripheral skin RTT's. The time required for outer shell temperature stability was arbitrarily defined as the elapsed time when the rate of change of the average of the three outer shell temperatures (excluding the vent port RTT) was less than 1° F per 5 hours.

g. Environmental temperature changes were made in 70° F increments throughout the program. Approximately 3 hours were required to establish stable environmental conditions.

The external insulation thermal performance test is graphically summarized by figure 13. This figure illustrates the heat leak versus environmental temperature; performance curves for 25, 50, and 100 layers of external insulation are included. Single point performance data are indicated for the non-insulated tests, the tests with 5 layers of insulation with vapor cooling, and the tests with 25 layers of insulation without vapor cooling. The heat leak value indicated by sequence 11 is apparently low due to a possible early termination of the sequence, therefore the curve fit for the 25 layer performance does not include the sequence 11 data point. Also included is the performance data from a previous test program (MSC-IN-66-EP-10) illustrating the non-insulated CSS performance in 50° to 150° F environments. The difference in the slope of the heat leak versus environmental temperature for the non-insulated and externally insulated CSS should be noted. The manufacturer of the CSS indicates that the predominant mode of heat transfer is radiation from the outer shell (approximately 90 percent). As the temperature of the CSS outer shell is reduced through the use of external insulation, the fourth power relationship of the radiant heat transfer results in a decreased slope of the heat leak versus environmental temperature curve. Sequences 5, 8, 11, and 13 were conducted in a 70° F environment with vapor cooling but with various thicknesses of external insulation. Sequence 3 was tested under identical conditions but with no external insulation. Using sequence 3 as baseline data the following percent reductions in heat leak were indicated: 50 layers —39.7 percent, 100 layers—50.5 percent, 25 layers—38.8 percent, and 5 layers —28.2 percent.

Figure 14 illustrates the heat leak versus insulation thickness. Three independent curves illustrate the performance in 0° F, 70° F, and 140° F environments. The decreasing effectiveness (percentagewise) of additional layers of insulation is readily apparent from this figure. The extension of the 140° F curve for a bare CSS is approximated from the prior test program data adjusted for expected vapor-cooled performance.

Figure 15a illustrates the temperature gradient through the external insulation versus the insulation thickness for 50 layers, figure 15b for 100 layers, and figure 15c for 5 and 25 layers. This temperature gradient was determined by the temperature sensors located on the outer shell of the CSS and between various layers of the laminar insulation. As the insulation thickness is increased the slope of the temperature gradient decreases, indicating the decreasing effectiveness of the additional layers of insulation. The average outer shell temperature is difficult to clearly define, because with external insulation a temperature gradient will exist around the outer shell. The lowest temperature will be near the vent port and the highest near the support points. The outer shell temperatures for all sequences were the average of 4 RTT's located as specified in the procedure. Since identical measurement points were used for all locations, these outer shell temperatures will serve well for comparative purposes. Based on this approach the minimum average outer shell temperature occurred with 100 layers of insulation, in a 0° F environment, and was -102° F. The maximum outer shell temperature noted during the external insulation testing was 26° F with 25 layers of insulation and in a 140° F environment.

Figure 16 illustrates the CSS outer shell temperature versus insulation thickness. The three curves illustrate the performance in 0° F, 70° F, and 140° F environments. The expected performance curves for the 0° F and the 140° F environments are projected below the 25 layer thickness. This again illustrates the diminishing effectiveness of the additional layers of insulation.

All test sequences in the vacuum environment, except sequences 2 and 9, were vapor cooled. These two sequences may be compared with the vapor-cooled sequences under similar conditions, in order to determine the effectiveness of vapor cooling. The effectiveness was limited in this application by the low specific heat of nitrogen, and by the fact that the CSS was not originally designed for vapor cooling. Therefore, the effectiveness may have been limited by the vent port design and the method of bonding the vapor cooling line to the outer shell. Sequence 2 (no vapor cooling) indicated a heat leak of 10.6 BTU/hour, whereas the corresponding sequence with vapor cooling, sequence 3, indicated a heat leak of 10.0 BTU/hour. Thus, heat leak was reduced 5.7 percent due to vapor cooling.

Sequence 9 and 11 may be compared as an indication of the effectiveness of vapor cooling with 25 layers of external insulation. The sequence 9 (non-vapor-cooled) heat leak was 7.1 BTU/hour, and the sequence 11 (vapor-cooled) heat leak was estimated to be 6.4 BTU/hour. (This sequence 11 value is derived from a curve fit, shown in figure 13, because as previously mentioned, the actual test value was apparently low due to a possible early termination of the sequence). Thus, the heat leak reduction due to vapor cooling was 9.6 percent (0.7 BTU/hour). The average outer shell temperature (excluding the vent port temperature) indicated 5° F decrease with vapor cooling (sequence 9 = -10.5° F and sequence 11 = -15.6° F). The calculated performance improvement due to vapor cooling, based on the vent port and the CSS outer shell temperature near the vapor cooling line termination, was found to be 0.5 BTU/hour. The difference between the apparent and calculated heat leak differential from vapor cooling may be due to the fact that the gas temperature was measured by a temperature sensor located near the exterior of the vent port. A more accurate means of determining the vapor cooling potential would be to locate temperature sensors directly in the vent gas stream at the start and end of the vapor cooling line.

The time required to achieve a steady state evaporation rate was considerably longer than that expected before the start of the program for the following reasons. In order to obtain useful evaporation rate data two conditions of equilibrium must be established. First, steady state temperatures must be obtained, and second, pressure-flow equilibrium must be established (that is, the CSS pressure or flow must increase or decrease to an equilibrium value corresponding to the steady state flow rate). The internal pressure of the CSS is a function of the pressure drop through the supply gas line, as the CSS pressure must be adequate to overcome the flow resistance of the supply gas piping system. The total test time for each sequence ranged from a minimum of 38 hours for sequence 2 to 206 hours for sequence 7.

The relationship between barometric pressure and flow rate fluctuations was recorded for the majority of the test sequences. Figure 12 illustrates a typical plot of flow rate and barometric pressure versus ET. As is apparent from the figure, the fluctuations in flow rate correspond to barometric pressure changes. The flow rate increases as the barometric pressure is decreasing, and the flow decreases as the barometric pressure is increasing.

In a CSS evaporation rate test a saturated liquid/vapor fluid exists, therefore, at any pressure, the fluid is at its corresponding saturation temperature. This results in a high thermodynamic inertia for pressure changes. Under steady-state conditions the CSS pressure is determined by the sum of the gas receiver pressure (the atmosphere for this test program) and the pressure drop through the vent system which is a function of the flow rate.

The CSS heat leak is essentially independent of changes in barometric pressure since the resultant minor changes in the fluid temperature have an insignificant effect. Under new steady state conditions, the flow rate will be essentially the same as the initial flow rate since the heat of vaporization and vapor density changes are insignificant for small pressure changes.

Due to the high thermodynamic inertia of the stored fluid, response of the CSS pressure to a change in receiver pressure is extremely slow. The net result of a change is a transient flow condition not truly representative of the heat leak of the CSS, since the transient flow rate is a function of the differential pressure between the CSS and the receiver. This effect is more pronounced as the ratio of fluid mass to heat leak increases. In future tests, this problem may be avoided by the use of a constant pressure receiver for the expelled gas.

Figure 17 illustrates the relationship of heat leak and outer shell temperature. The data scatter is probably due to the difficulty in accurately establishing the average CSS shell temperature due to the thermal gradients from the vent port to the support points. As is evident, it is extremely important to minimize the outer shell temperature, particularly in systems where radiative heat transfer is the prime mode of heat leak.

Detailed performance data for each sequence are included in the appendix. A temperature plot indicates all recorded temperatures at the end of each sequence. A curve of CSS temperatures and evaporation rate versus ET indicates performance throughout each of the test sequences.

Decompression Test

Two decompression tests were conducted: one with 100 layers of insulation (sequence 1), and one with 25 layers of insulation (sequence 2). The rate of decompression for sequences 1 and 2 is illustrated in figure 18. For each decompression sequence, motion pictures of the CSS were taken from three views. For

both the 100-layer and 25-layer sequences, slight flexing of the insulation was noted during the first 5 seconds of decompression. No motion was noted during the remainder of the decompression.

The altitude chamber pressure and the pressure below the first layer of external insulation (next to the CSS outer shell) were recorded on an analog recorder during the decompression tests. No measurable pressure differential across the insulation was noted. The rate of decompression does not meet the Saturn V launch profile but was the maximum obtainable with existing facility equipment. No attempt was made to provide gas flow passages through the insulation. As described in the procedure, a rectangular sheet of insulation was cut to conform to the spherical configuration, the loose ends taped together and to the lower layer of insulation. The joints were not heat sealed or continously taped. This insulation technique apparently provided an adequate gas escape path to prevent gas entrapment and subsequent insulation rupture. It is recommended that additional effort be expended to investigate the behavior of external insulation under vibration and acceleration. No attempt was made to determine thermal performance after rapid decompression during this test program. This is also an area where additional testing is recommended.

General Comments

The most difficult problem faced during this program was that of defining and recognizing steady state flow conditions in order to terminate a test sequence. Some of the problems have been mentioned previously but are worth reiterating. In general, the conditions and/or problems associated with obtaining and recognizing stable flow are as follows:

a. Thermal stability of the outer shell must be established. Obviously, this cannot be accomplished unless stable environmental conditions are maintained for a significant time period. The definition of thermal stability must also be tempered by the location and accuracy of temperature measurement instrumentation.

b. During vented weight loss tests, the differential pressure (CSS to atmospheric) through the vent system is extremely small (0.4 to 2.4 psig). As a result, barometric pressure changes will significantly affect flow until a compensated CSS pressure can be established. Barometric pressure changes up to 0.0245 psi/hour were noted during these tests. In order to eliminate the effects of ambient pressure fluctuations on recorded flows, the system should be vented to a constant pressure receiver system. The CSS pressure should be measured with an absolute pressure transducer, rather than a psig transducer, so that the CSS pressure measurements are uneffected by atmospheric pressure changes.

c. Flow meter accuracies and stability are also extremely important in the low flow regimes experienced. Redundant flow measurement is definitely recommended, and flowmeter full scale ranges should be as close to the contemplated flow as is practical. As is the case with thermal stability, the definition of steady state flow must take into consideration the flow measurement equipment.

d. With proper instrumentation and calibration techniques, temperature data within $\pm$ 1° F and flow data that is $\pm$ 1 percent full scale are reasonably attainable. With these assumptions, continued effort should be expended to establish firm procedures and/or criteria for conducting vented weight loss heat leak evaluations.

CONCLUSIONS AND RECOMMENDATIONS

a. The use of the external laminar insulation in a vacuum environment resulted in a significant improvement in CSS thermal performance. A 51 percent reduction in heat leak was indicated with 100 layers of insulation; an appreciable reduction in heat leak (28 percent) was achieved with 5 layers of external insulation.

b. The CSS thermal performance improvement with external insulation is significant since the insulation may be applied to existing CSS designs, is inexpensive, and installation techniques do not appear to be a significant problem.

c. For maximum effectiveness of the external insulation, the CSS mounting structure should thermally isolate the CSS outer shell from the spacecraft structure. The test setup used in this program was designed to minimize conduction paths from the surroundings.

d. For maximum system performance, an adequate time period must be allowed for the externally insulated CSS to reach thermal equilibrium after being exposed to the vacuum environment.

e. The successful use of external insulation in a high-vacuum environment indicates that some of the complexities of previous CSS may be deleted (internal laminar insulation, radiation shields, internal vapor cooling, et cetera). The performance requirements of the vacuum annulus portion of CSS would be based on prelaunch hold requirements. Supplemental external insulation, which is effective only under vacuum conditions, would be used to meet mission minimum flow rate requirements.

f. The performance of external insulation under conditions of rapid decompression, vibration, and acceleration should be further investigated.

g. Vapor cooling does appear to be a further means of heat leak reduction, based on the limited comparative data obtained. More conclusive work should be done to establish the absolute value of this technique.

h. Stabilization requirements are a subject open to debate. More analyses and tests should be conducted to establish standardized stabilization criteria.

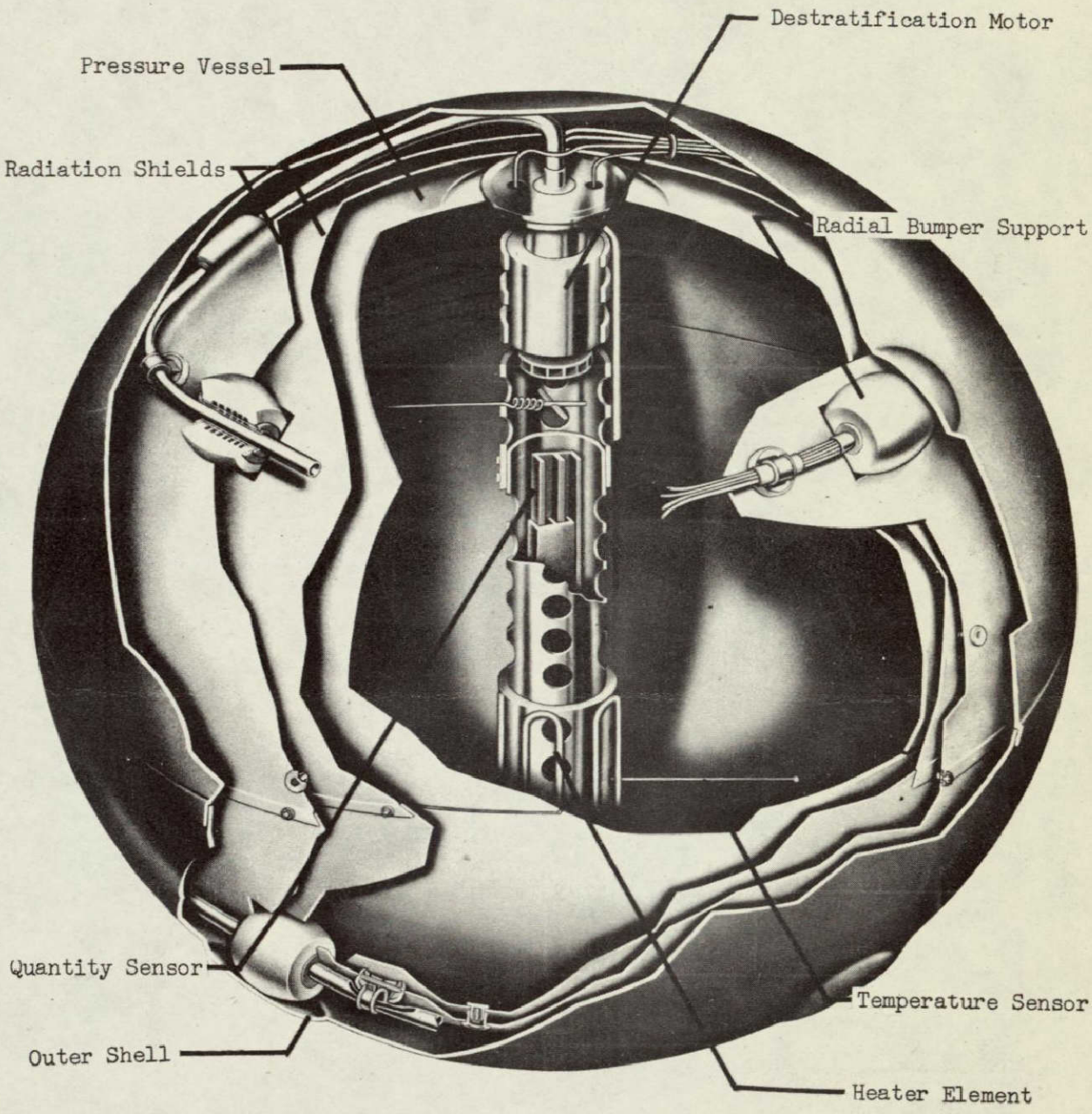

Figure 1.- Bendix "Phase-B" cryogenic storage system.

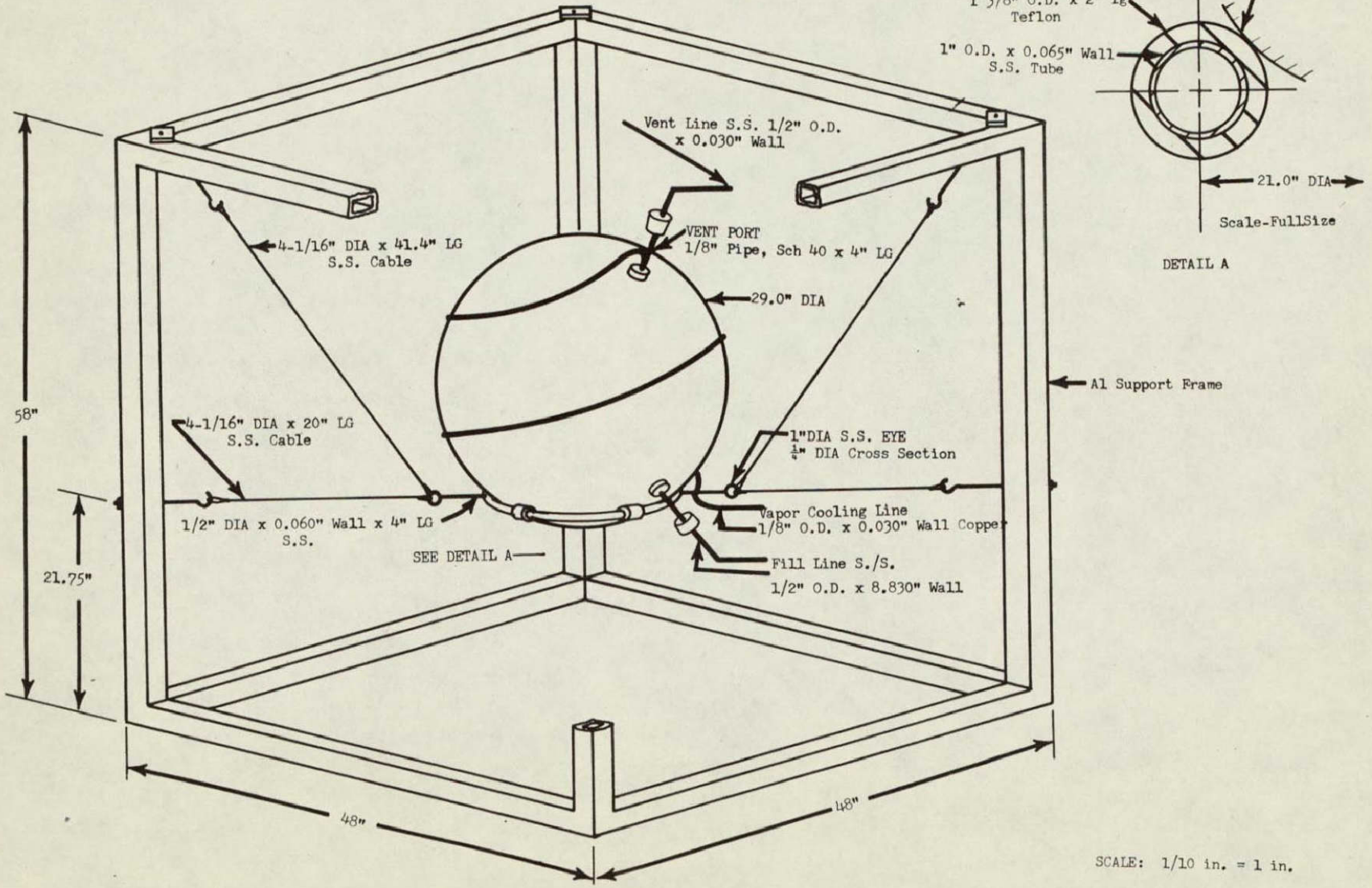

Figure 2.- Test support fixture.

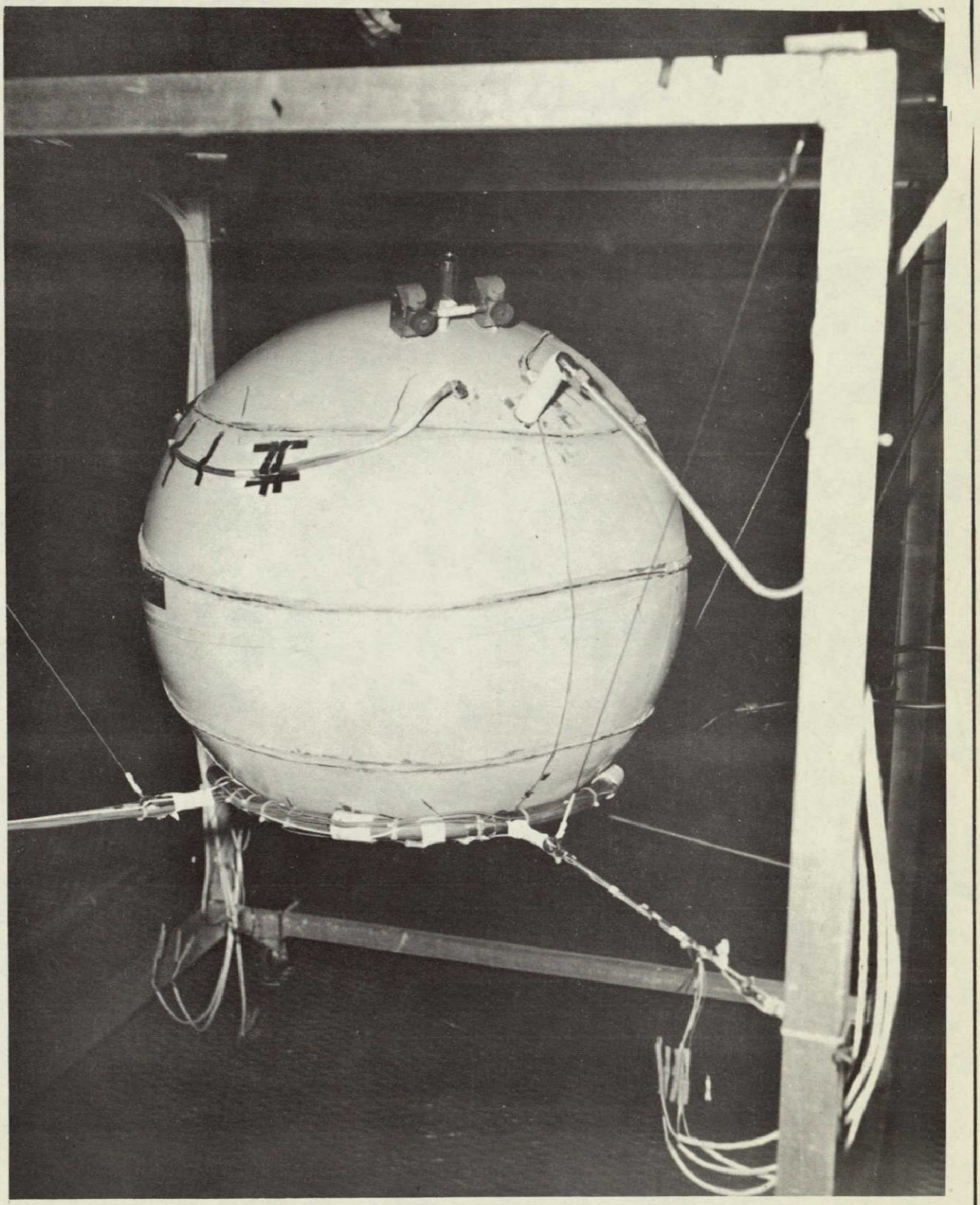

Figure 3.- Overall view of non-insulated CSS showing vapor cooling line installation.

Figure 4.- Initial wrap of rectangular sheet of laminar insulation.

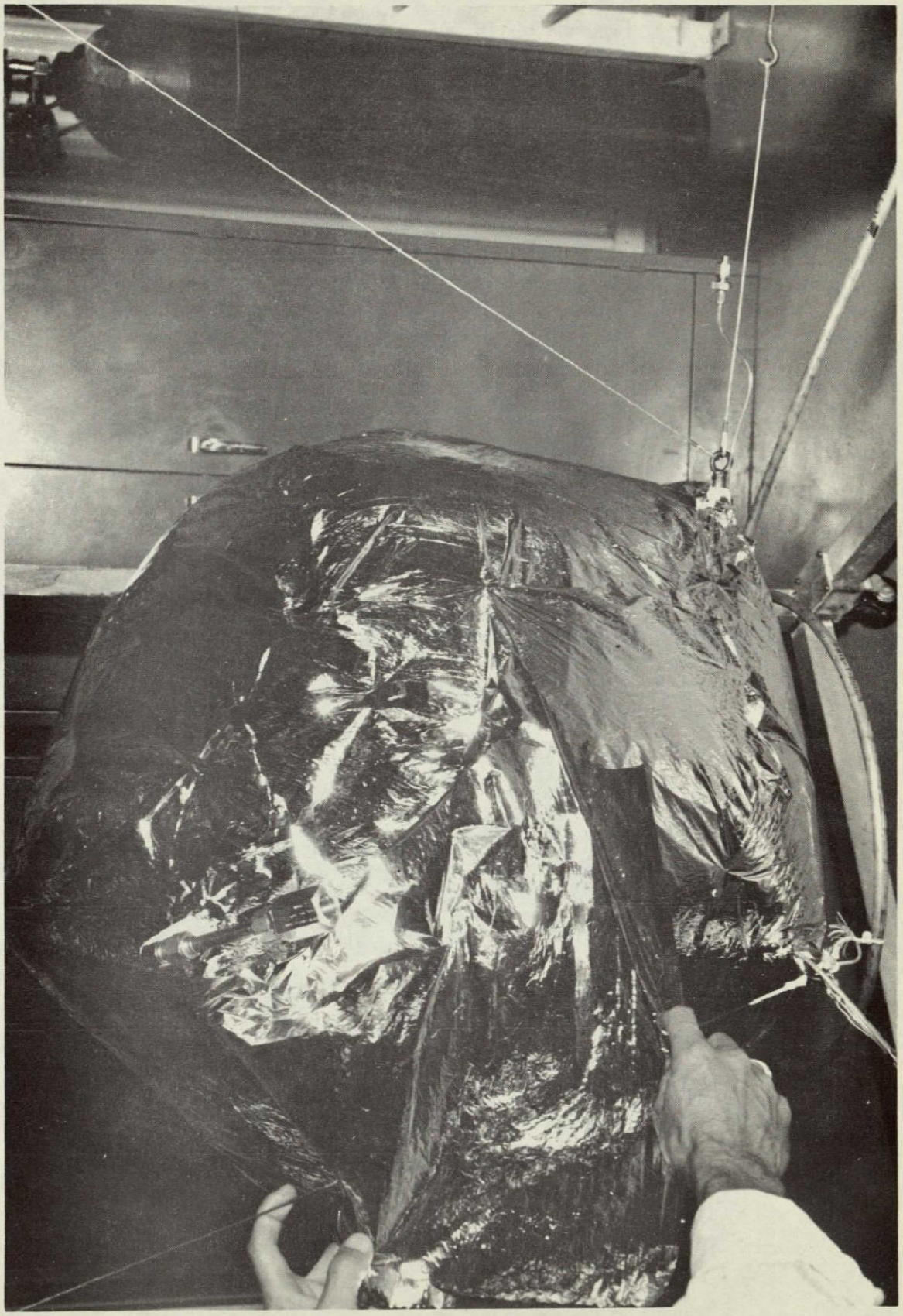

Figure 5.- Final forming of a sheet of laminar insulation.

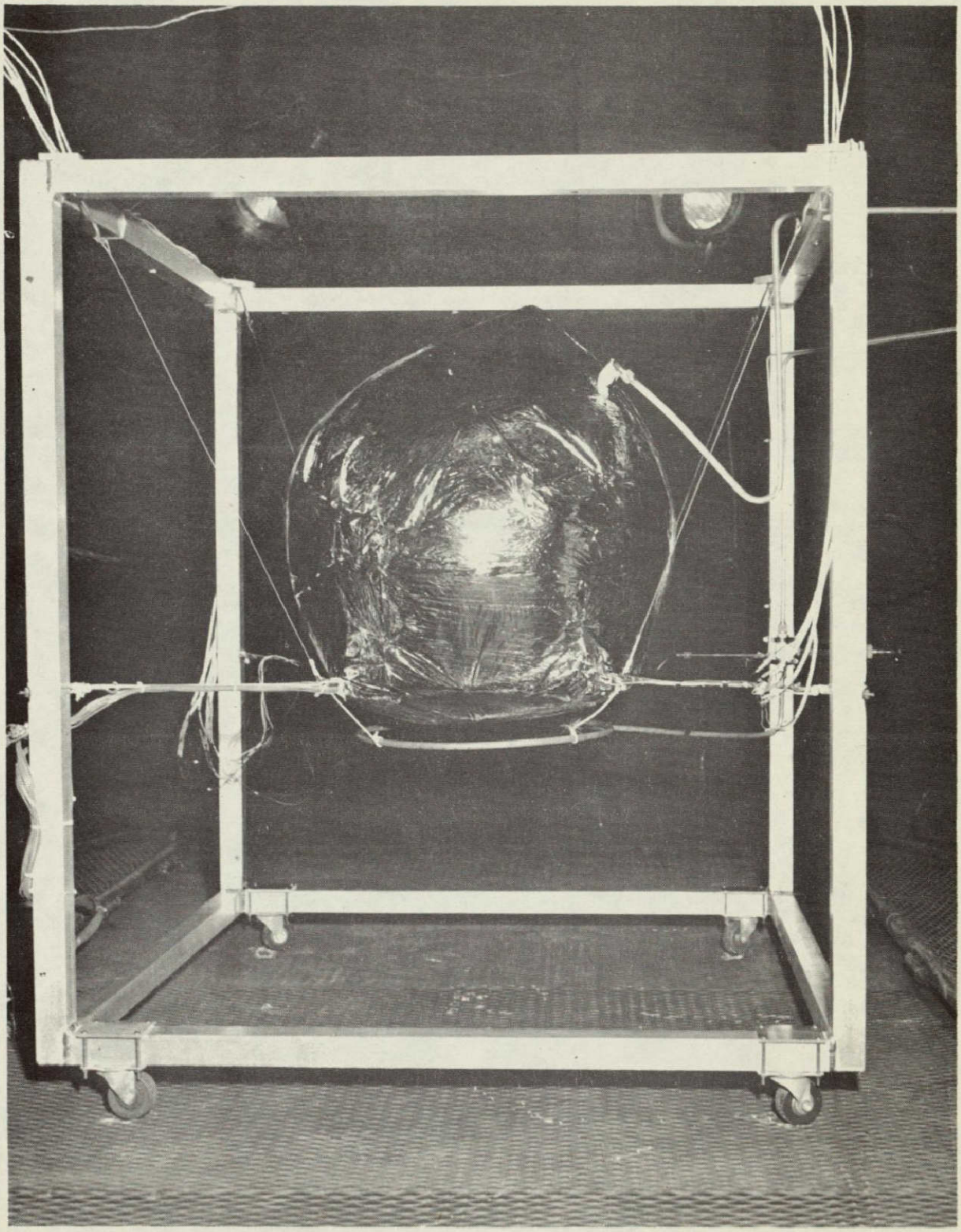

Figure 6.- Overall view of insulated CSS.

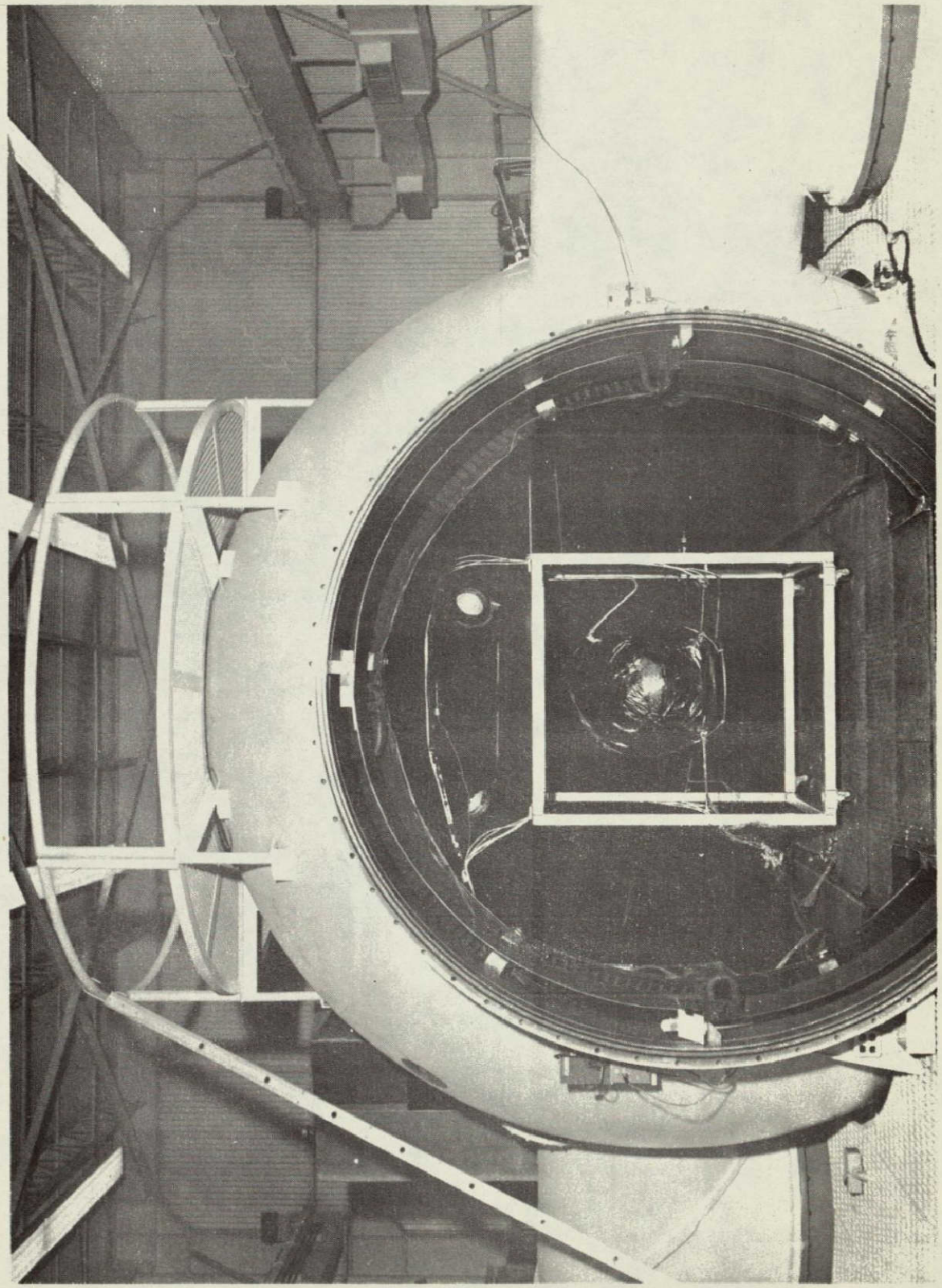

Figure 7.- Test fixture and CSS located in thermal vacuum chamber.

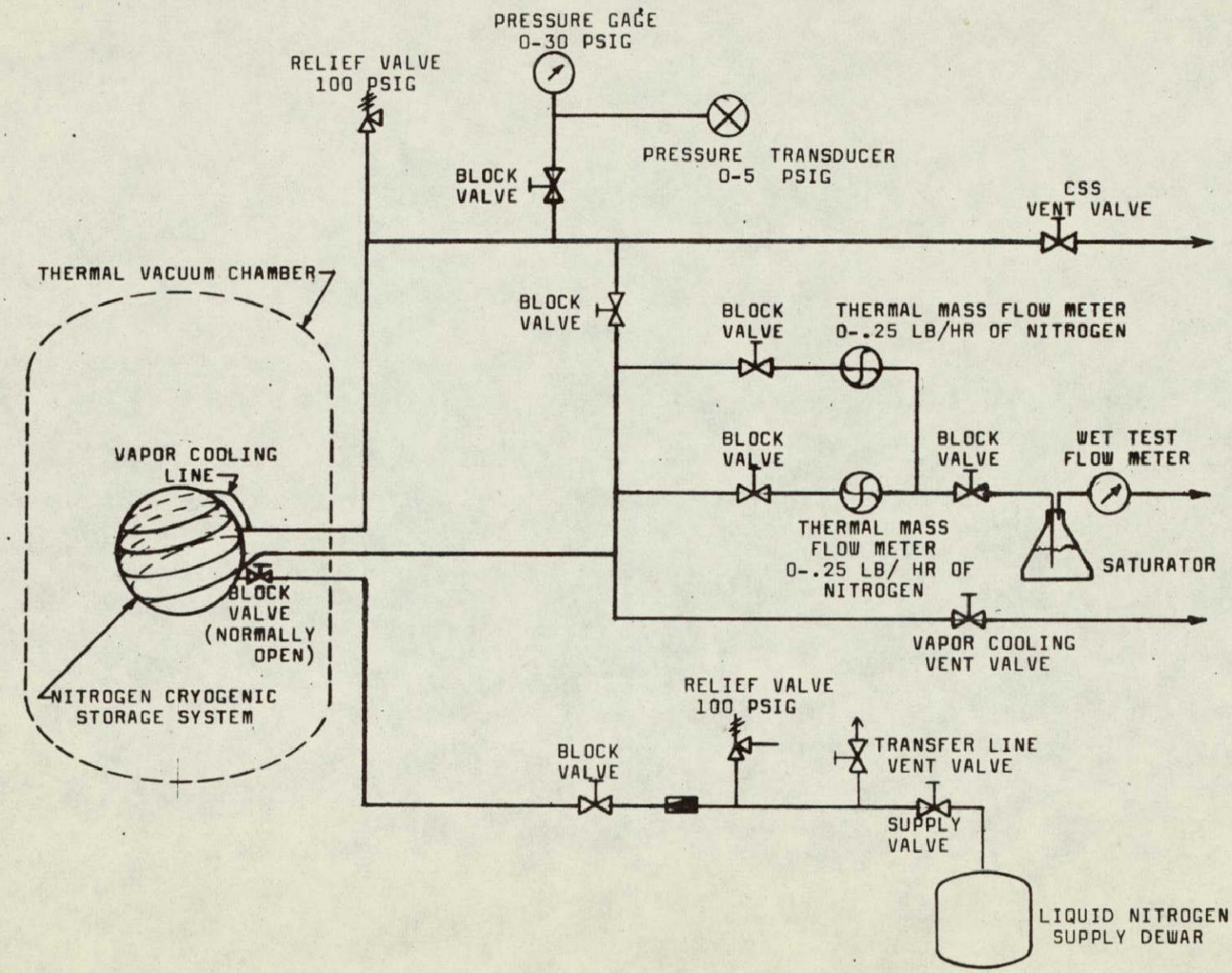

Figure 8.- Liquid transfer and gas flow system schematic.

DOC. NO. MSC-EP-R-67-15
REVISION New
PAGE 22 OF 35

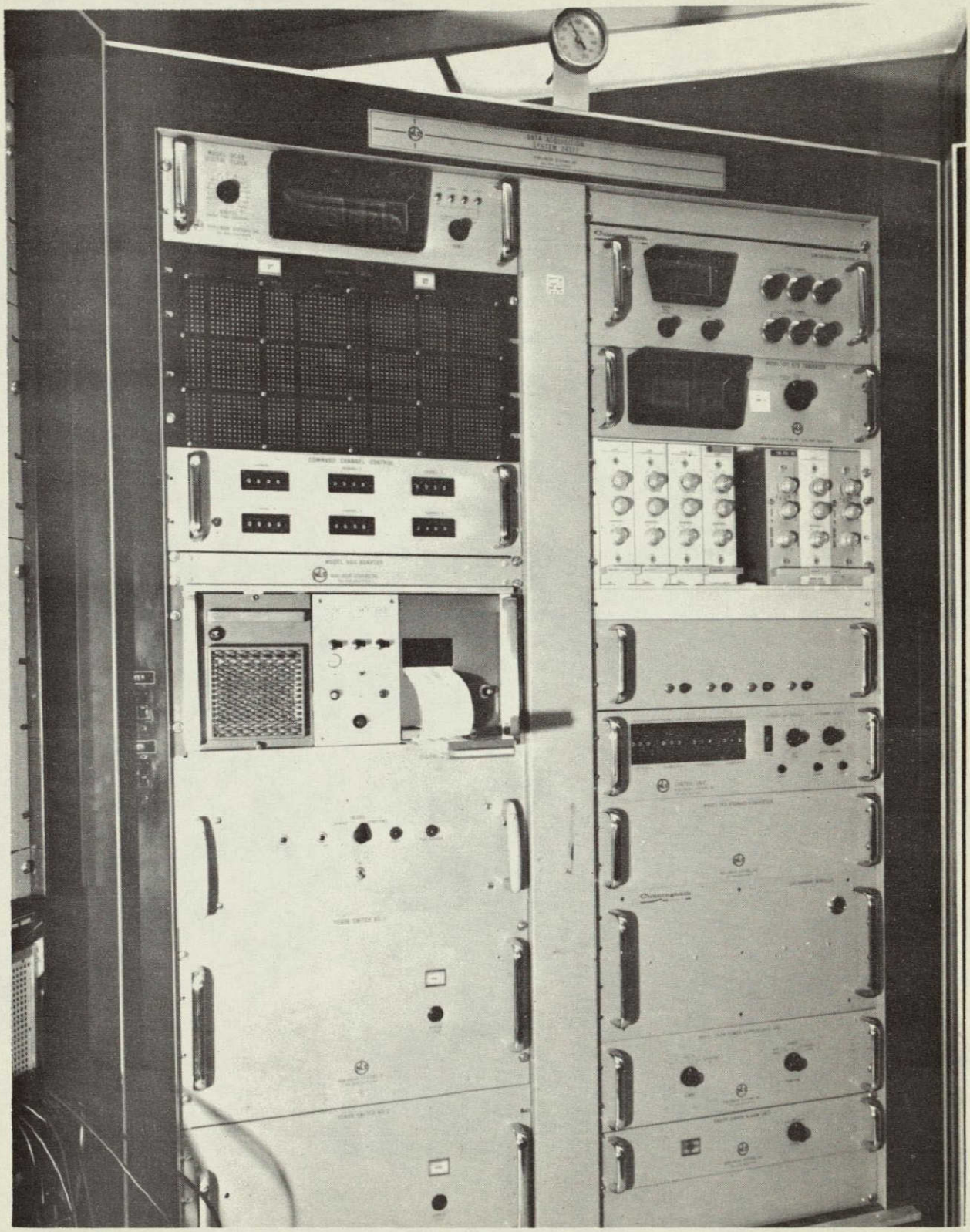

Figure 9.- Digital data acquisition system.

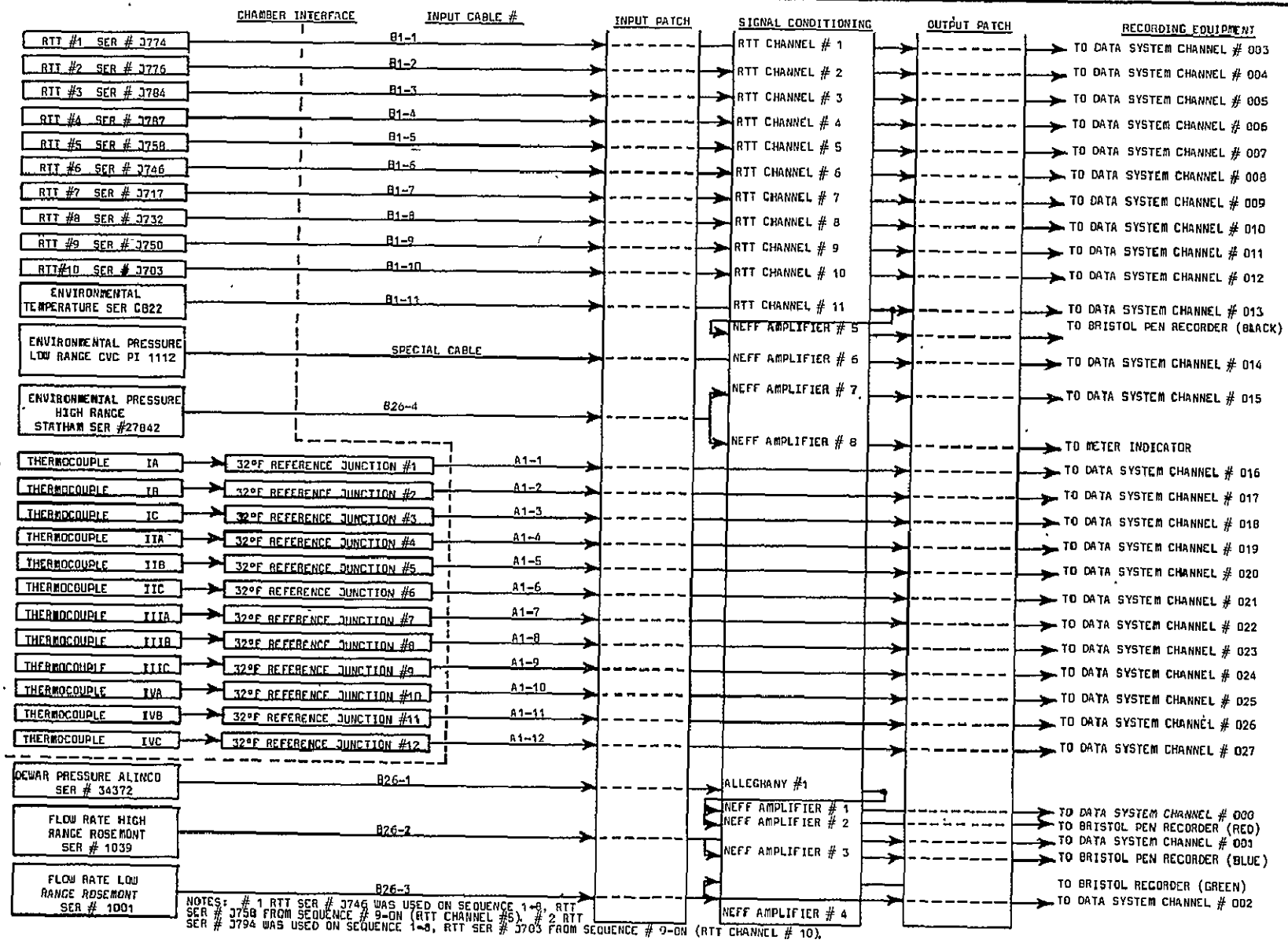

Figure 10.- Instrumentation and data acquisition system schematic.

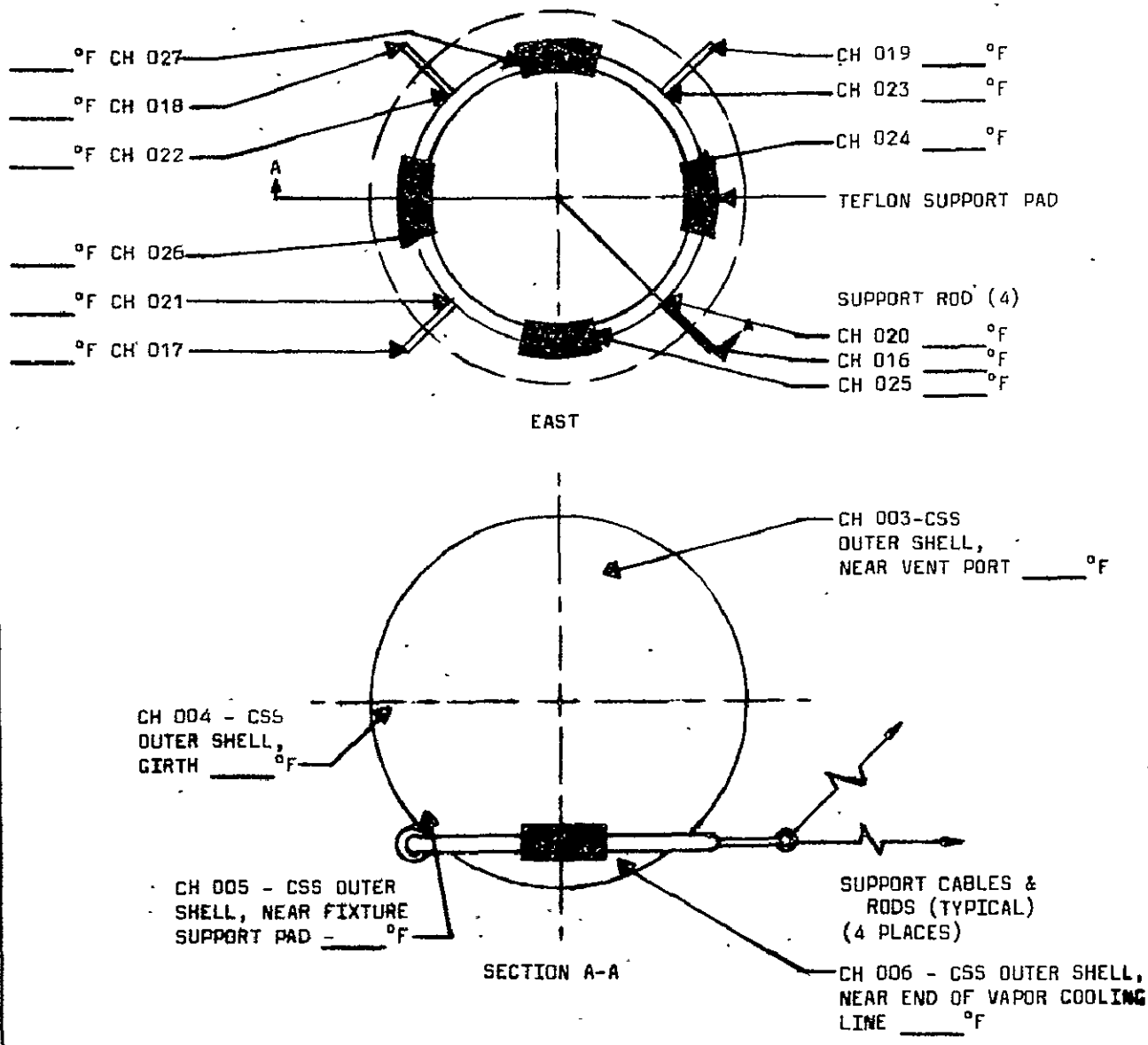

Figure 11.- Location of temperature sensors.

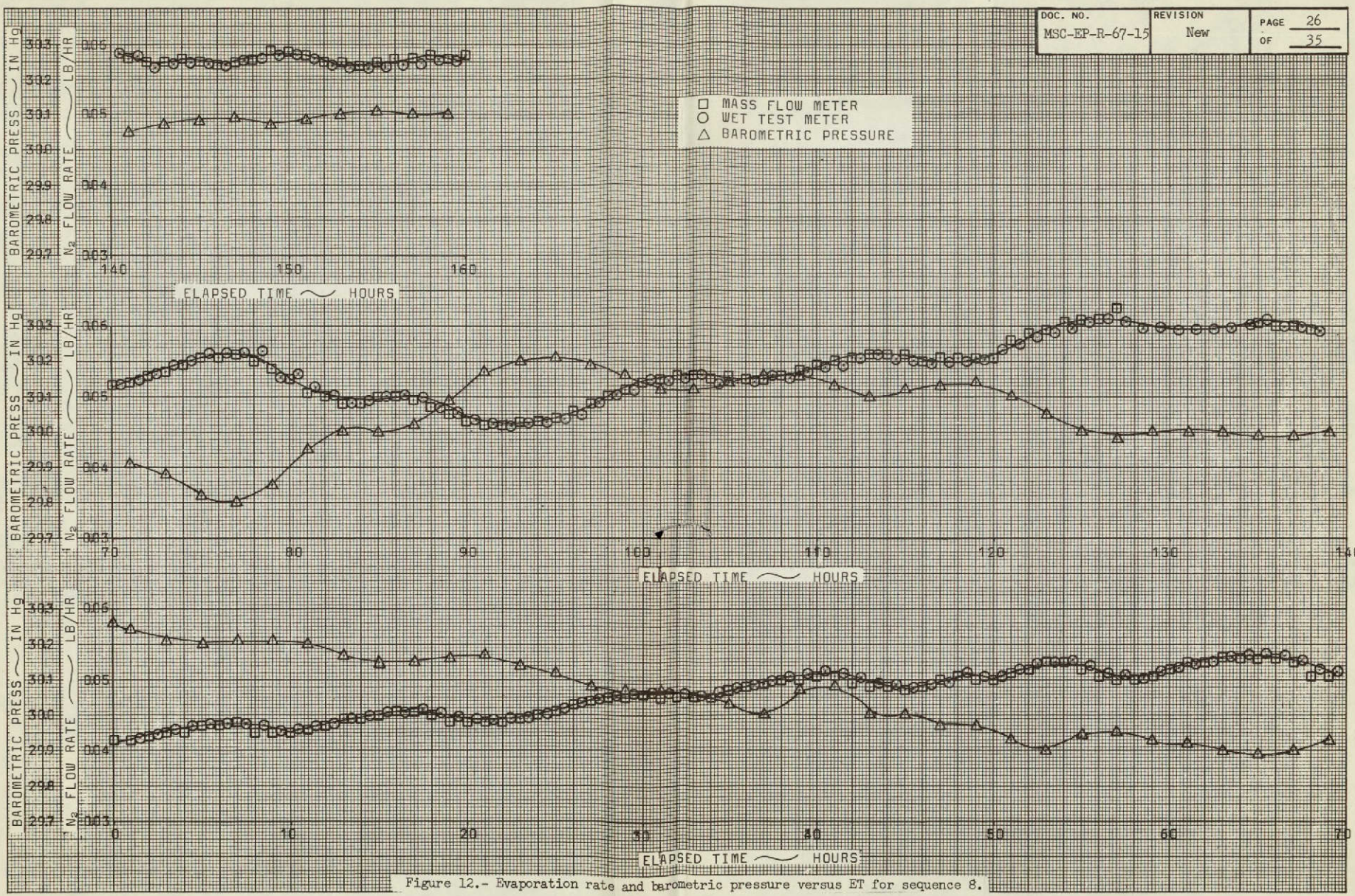

Figure 12.- Evaporation rate and barometric pressure versus ET for sequence 8.

FOLDOUT FRAME 1

FOLDOUT FRAME 2

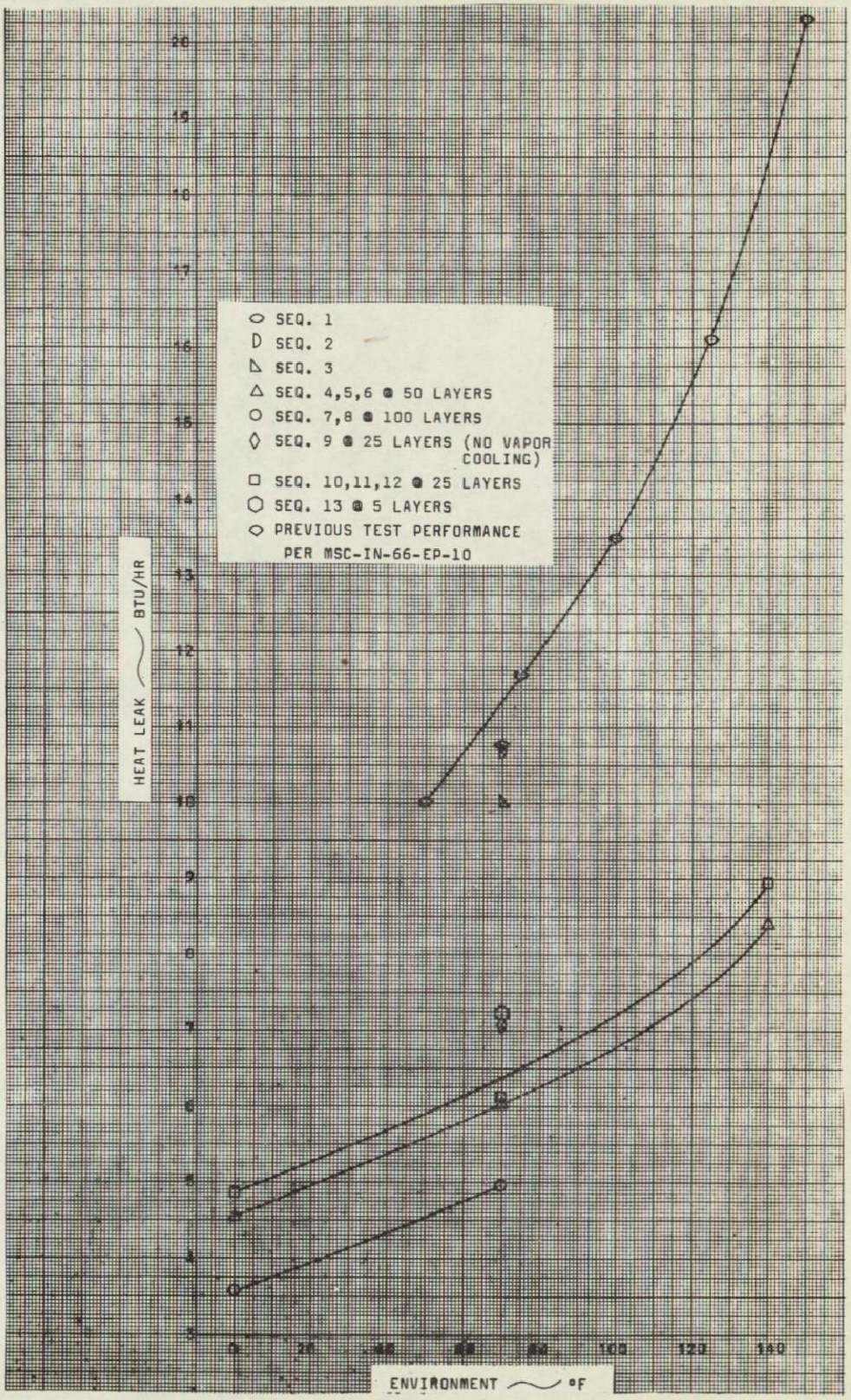

Figure 13.- Heat leak versus environmental temperature for 0, 5, 25, 50, and 100 layers of external insulation.

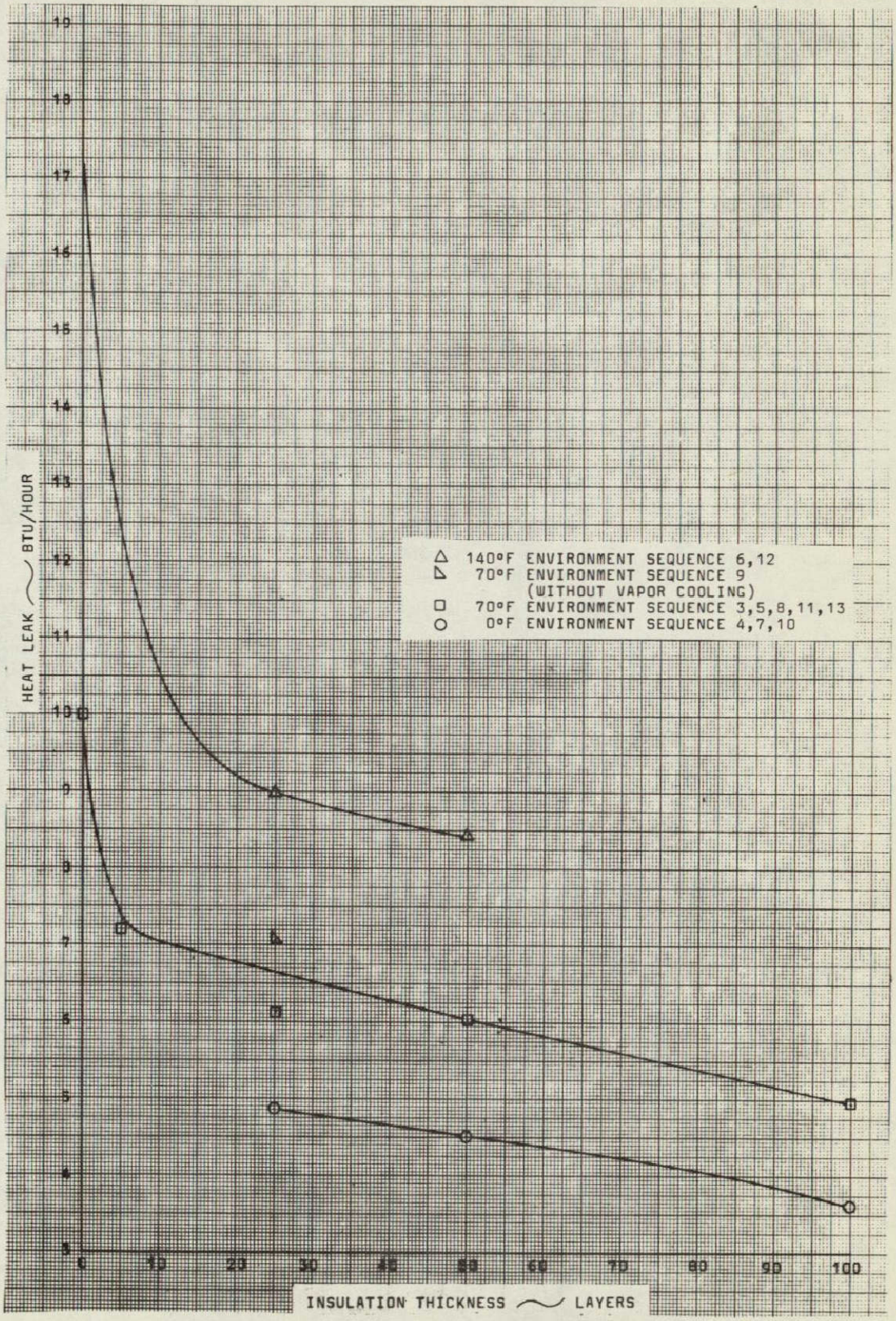

Figure 14.- Heat leak versus insulation thickness for 0° F, 70° F, and 140° F.

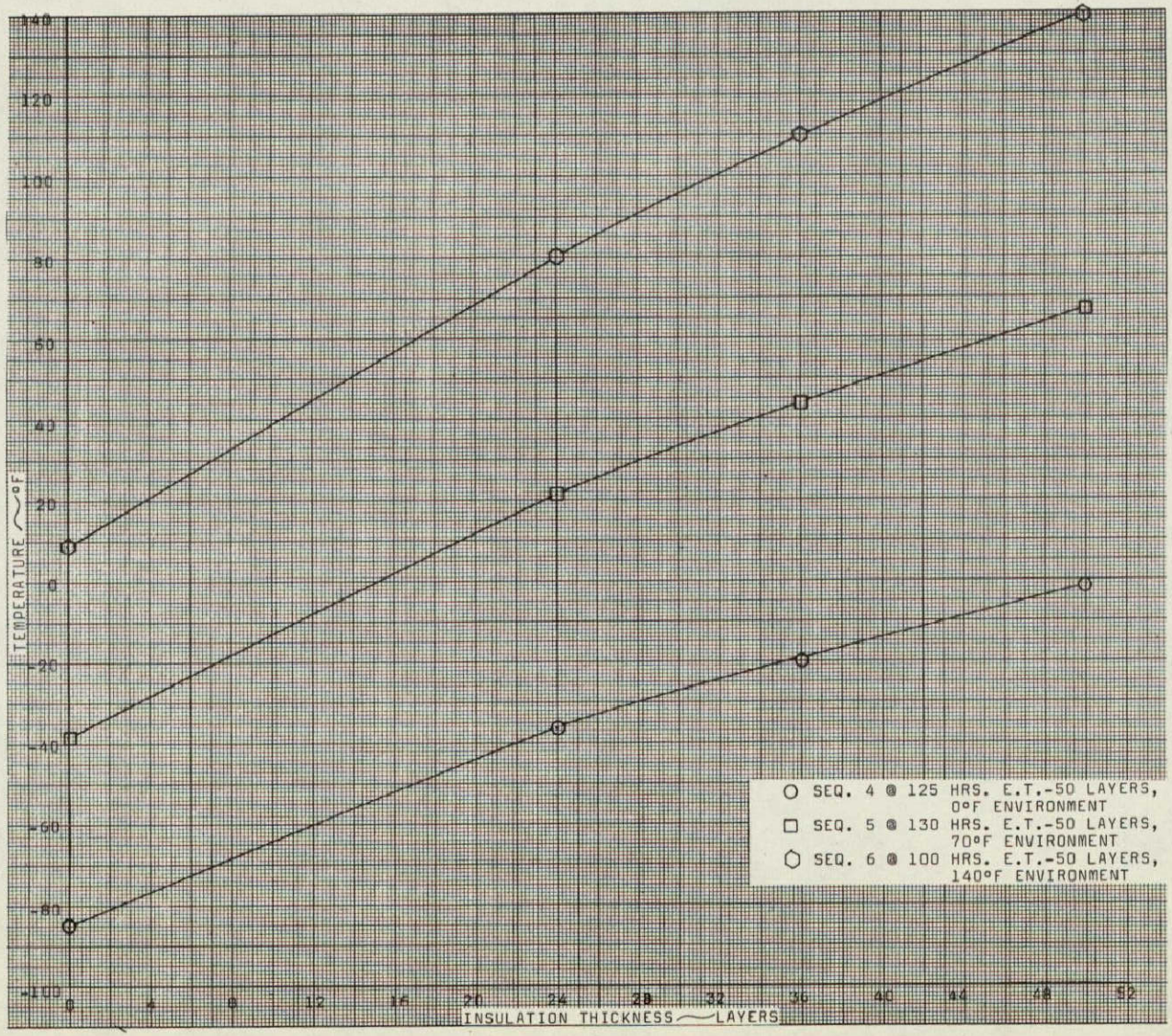

Figure 15a.- Temperature gradient versus insulation thickness for 50 layers of insulation.

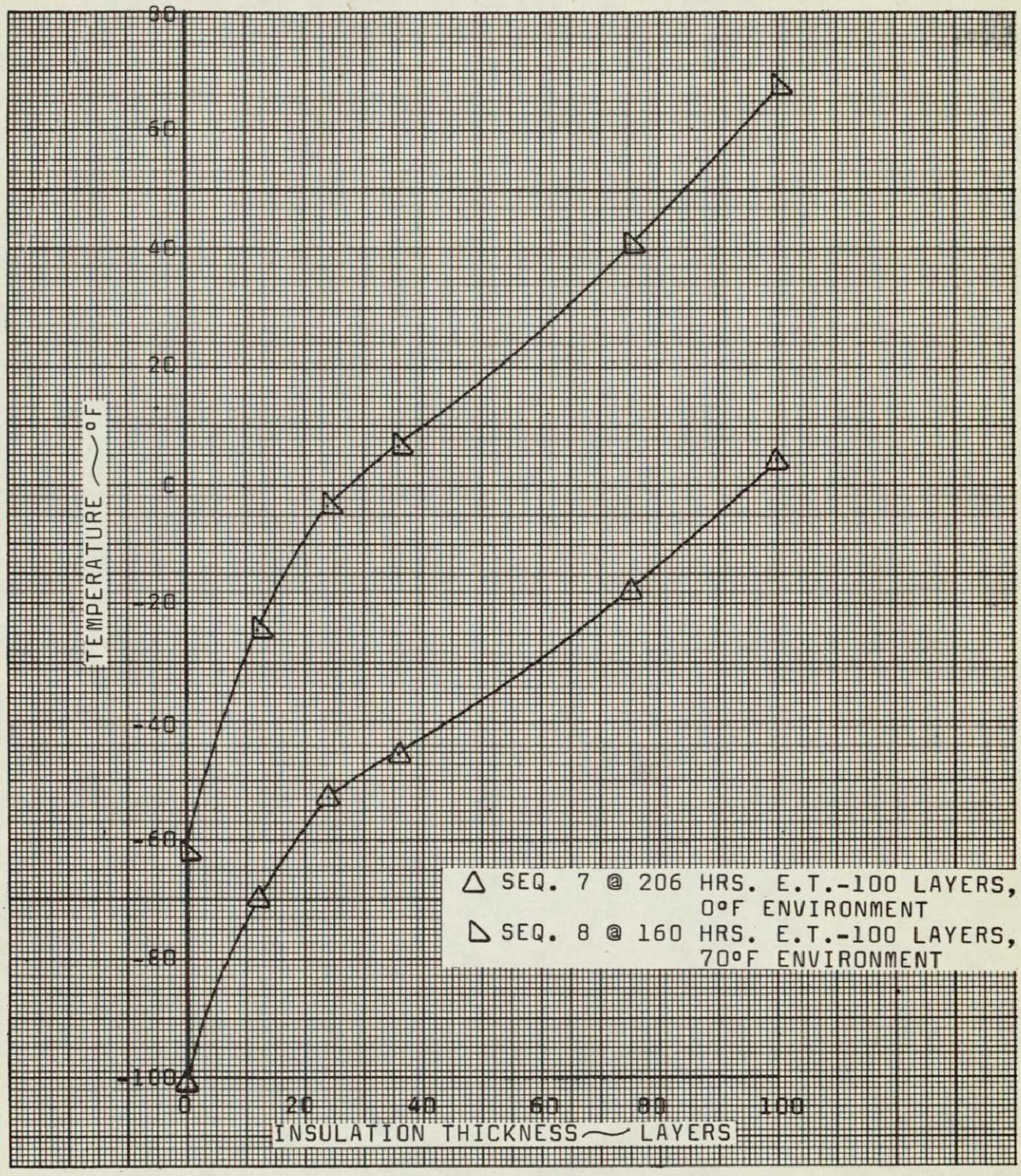

Figure 15b.- Temperature gradient versus insulation thickness for 100 layers of insulation.

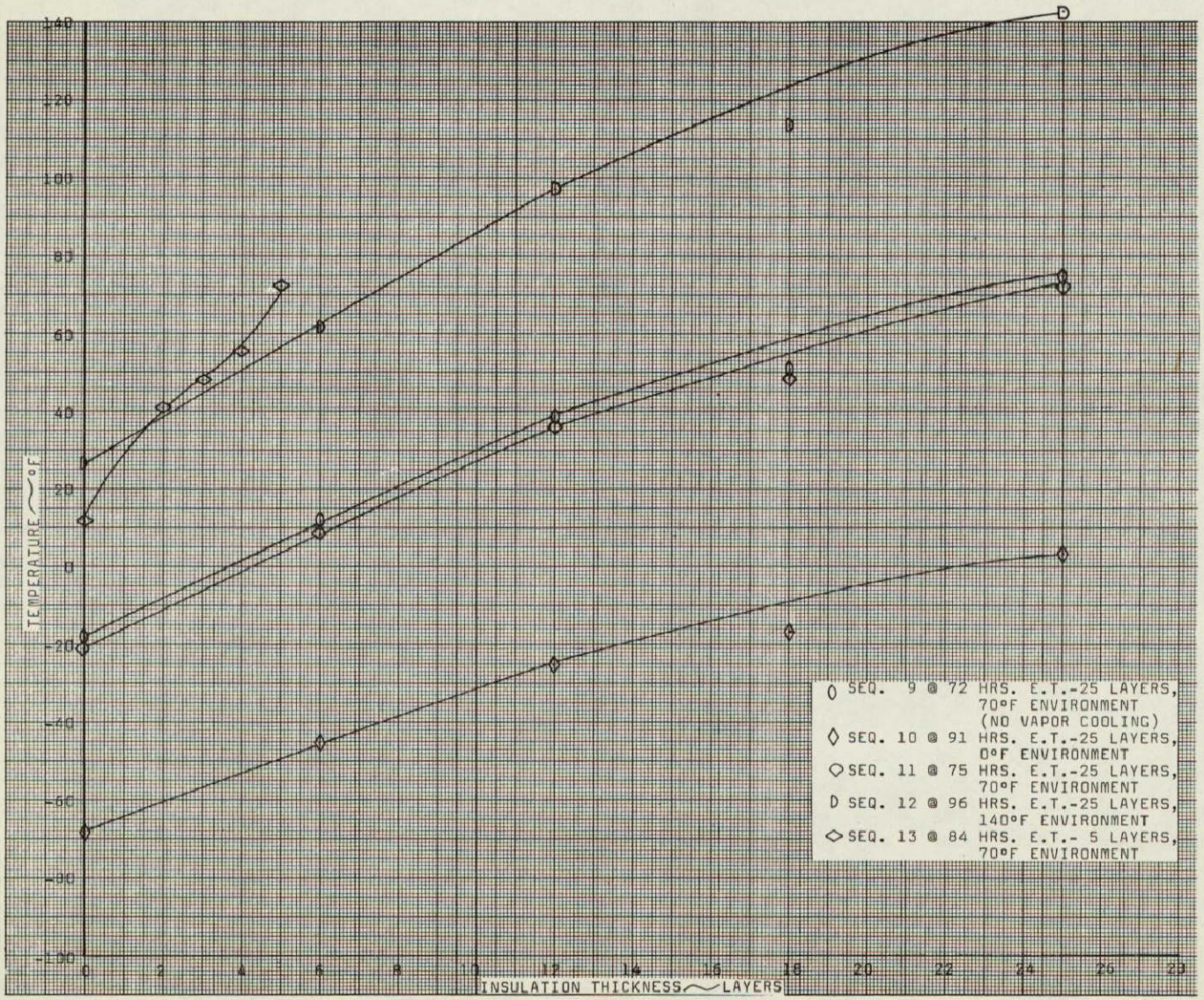

Figure 15c.- Temperature gradient versus insulation thickness for 25 and 5 layers of insulation.

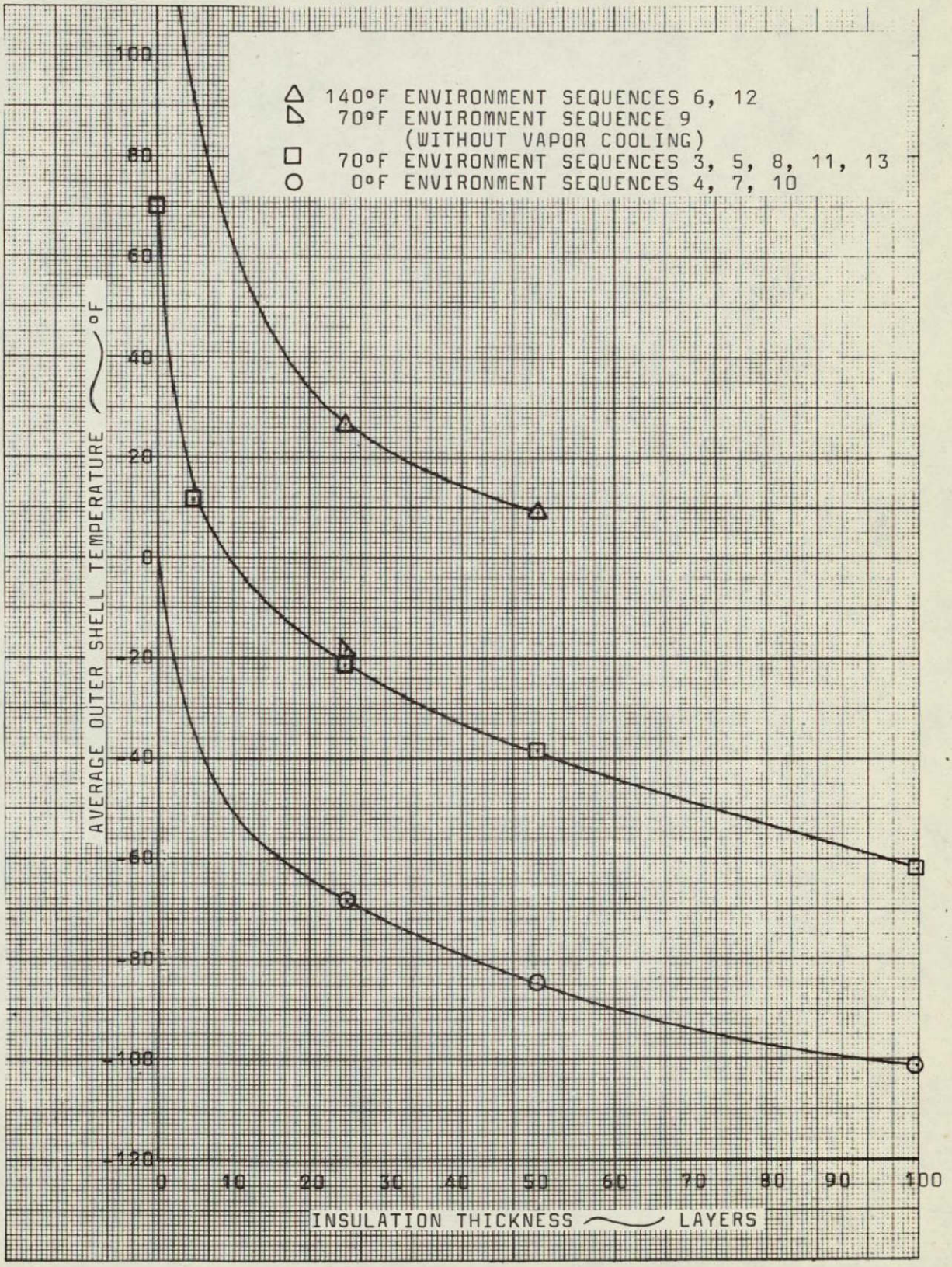

Figure 16.- CSS outer shell temperature versus insulation thickness.

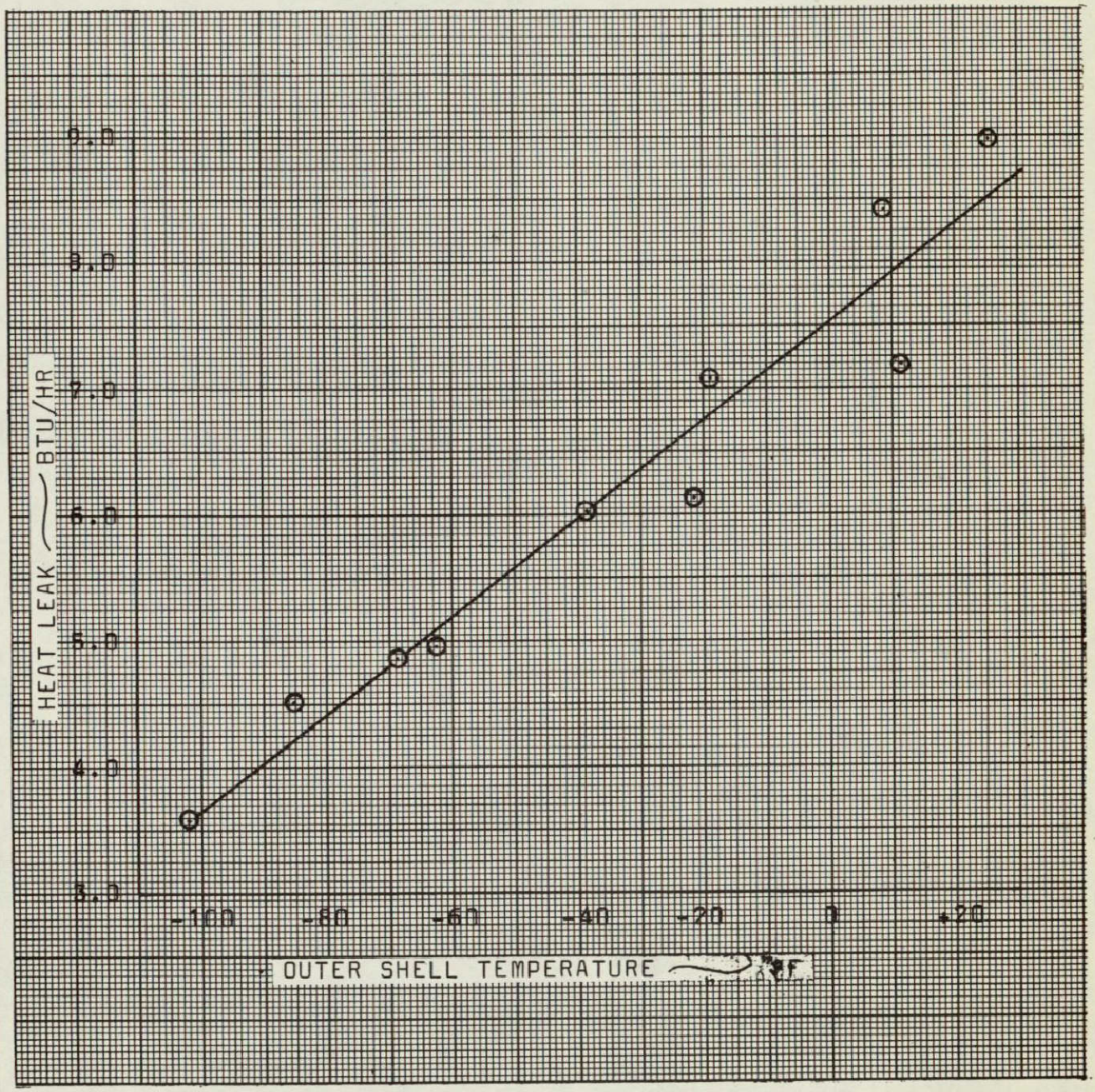

Figure 17.- Heat leak versus CSS outer shell temperatures.

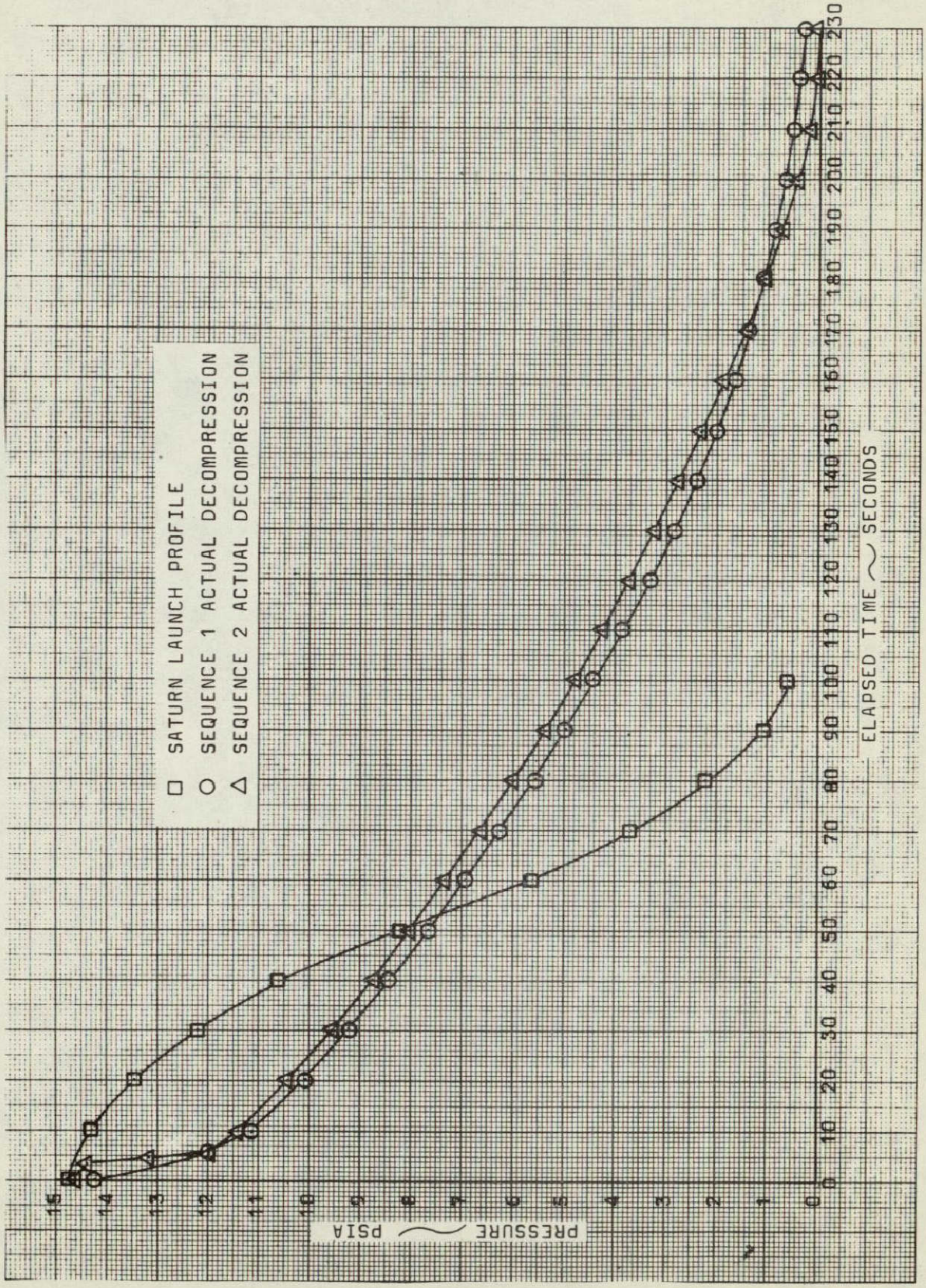

Figure 18.- Sequences 1 and 2 decompression.

MSC FORM 360B (JAN 67)

TABLE I.-EXTERNAL INSULATION TEST

SEQUENCE NUMBER	EXTERNAL INSULATION	VAPOR COOLING	ENVIRONMENT	N_2 EVAPORATION	CSS PRESSURE	HEAT LEAK	TOTAL TEST TIME	ELAPSED TIME FOR EVAPORATION RATE AVERAGE	TOTAL VARIATION DURING EVAPORATION RATE ELAPSED TIME	OUTER SHELL TEMPERATURE STABILITY ELAPSED TIME	OUTER SHELL AVG. TEMPERATURE AT TOTAL TEST TIME
	LAYERS			LB/HR	PSIG	BTU/HR	HR	HR	LB/HR	HR	°F
1	NONE	NO	70°F AMBT. PRESS.	0.126	0.97	10.77	56	50-55	.1260 / .1265	N/A	64.5
2	NONE	NO	70°F VACUUM	0.125	1.01	10.62	38	30-35	.1250 / .1255	N/A	68.2
3	NONE	YES	70°F VACUUM	0.1180	2.38	10.01	72	60-70	.1175 / .1185	N/A	63.9
4	50	YES	0°F VACUUM	0.0528	0.60	4.51	127	115-125	.0545 / .0515	100	-85.1
5	50	YES	70°F VACUUM	0.0708	1.05	6.04	130	120-130	.0711 / .0705	75	-38.7
6	50	YES	140°F VACUUM	0.0988	1.63	8.41	100	90-100	.0990 / .0975	50	9.0
7	100	YES	0°F VACUUM	0.0419	0.46	3.58	206	195-205	.0430 / .0400	110	-102.0
8	100	YES	70°F VACUUM	0.0580	0.70	4.95	160	150-160	.0590 / .0570	85	-62.2
9	25	NO	70°F VACUUM	0.0828	0.57	7.08	72	60-70	.0840 / .0815	50	-18.9
10	25	YES	0°F VACUUM	0.0575	0.72	4.86	90	80-90	.0580 / .0560	75	-68.6
11	25	YES	70°F VACUUM	0.0719	1.07	6.13	75	70-75	.0720 / .0718	60	-21.4
12	25	YES	140°F VACUUM	0.1055	1.84	8.97	96	85-95	.1050 / .1060	55	26.6
13	5	YES	70°F VACUUM	0.0844	1.42	7.19	86	70-80	.0837 / .0850	55	11.5

APPENDIX

PERFORMANCE DATA

TABLE OF CONTENTS

SEQUENCE: 1
ELAPSED TIME: 56 hours

EXTERNAL INSULATION: 0 (zero) LAYERS
ENVIRONMENTAL TEMP: 72.4 °F

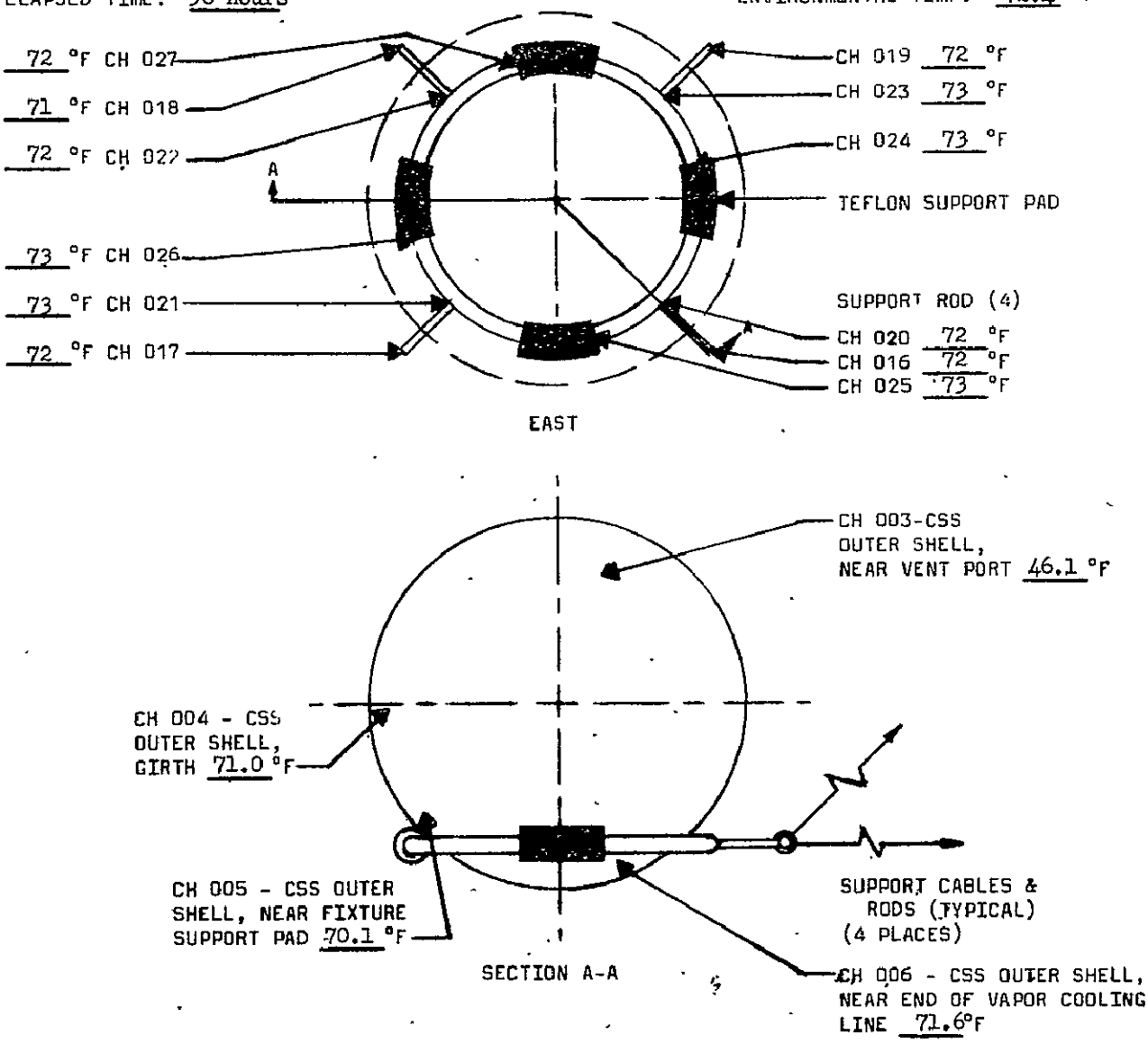

Average Temperature of Outer Shell (Channels 003, 004, 005, and 006) 64.7°F.

Sequence 1 final temperature plot.

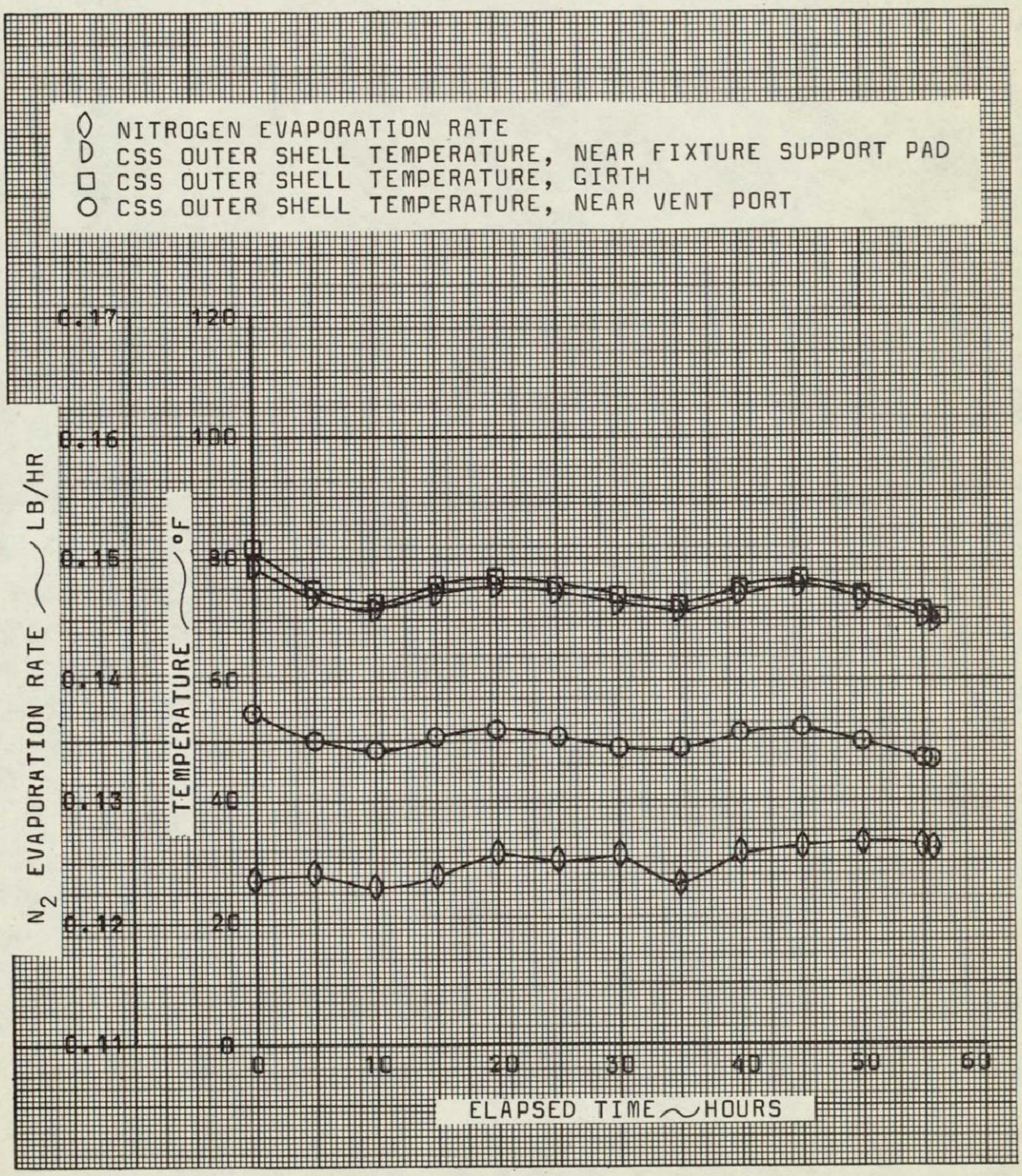

Sequence 1 CSS temperature and evaporation rate versus ET.

SEQUENCE: 2
ELAPSED TIME: 38 hours

EXTERNAL INSULATION: 0 LAYERS
ENVIRONMENTAL TEMP: 76.1 °F

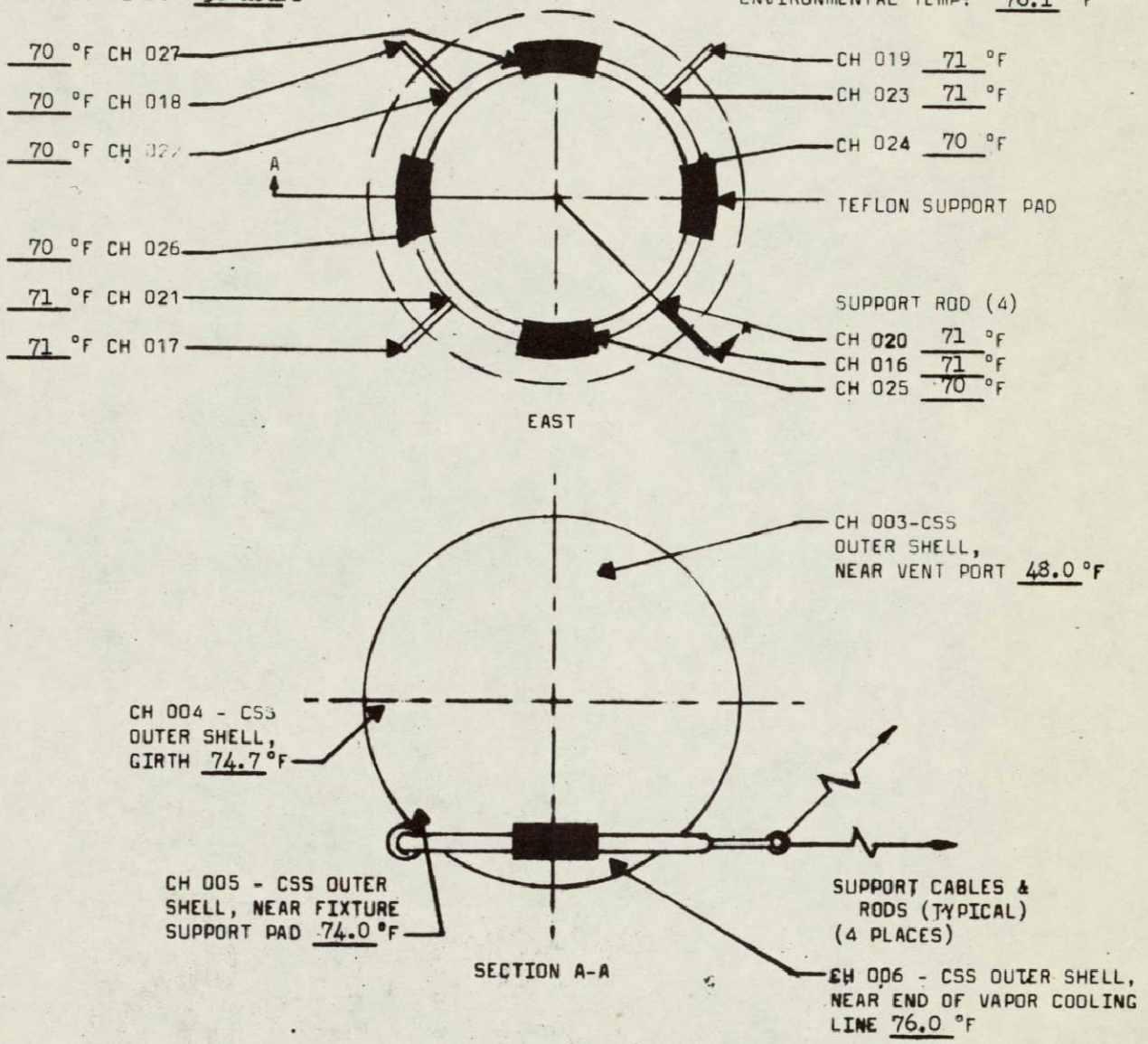

Average Temperature of Outer Shell (Channels 003, 004, 005, and 006) 68.2°F.

Sequence 2 final temperature plot.

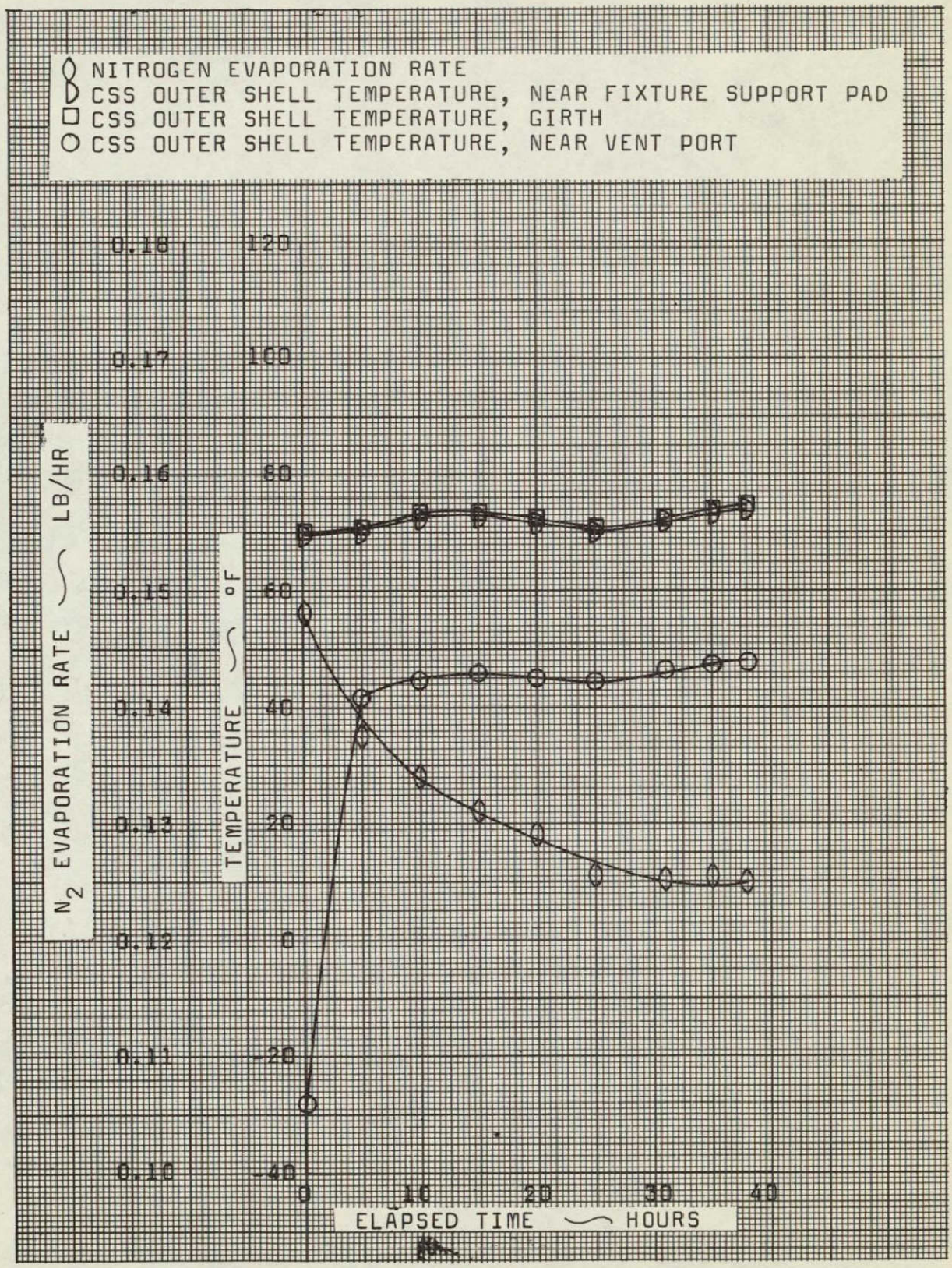

Sequence 2 CSS temperature and evaporation rate versus ET.

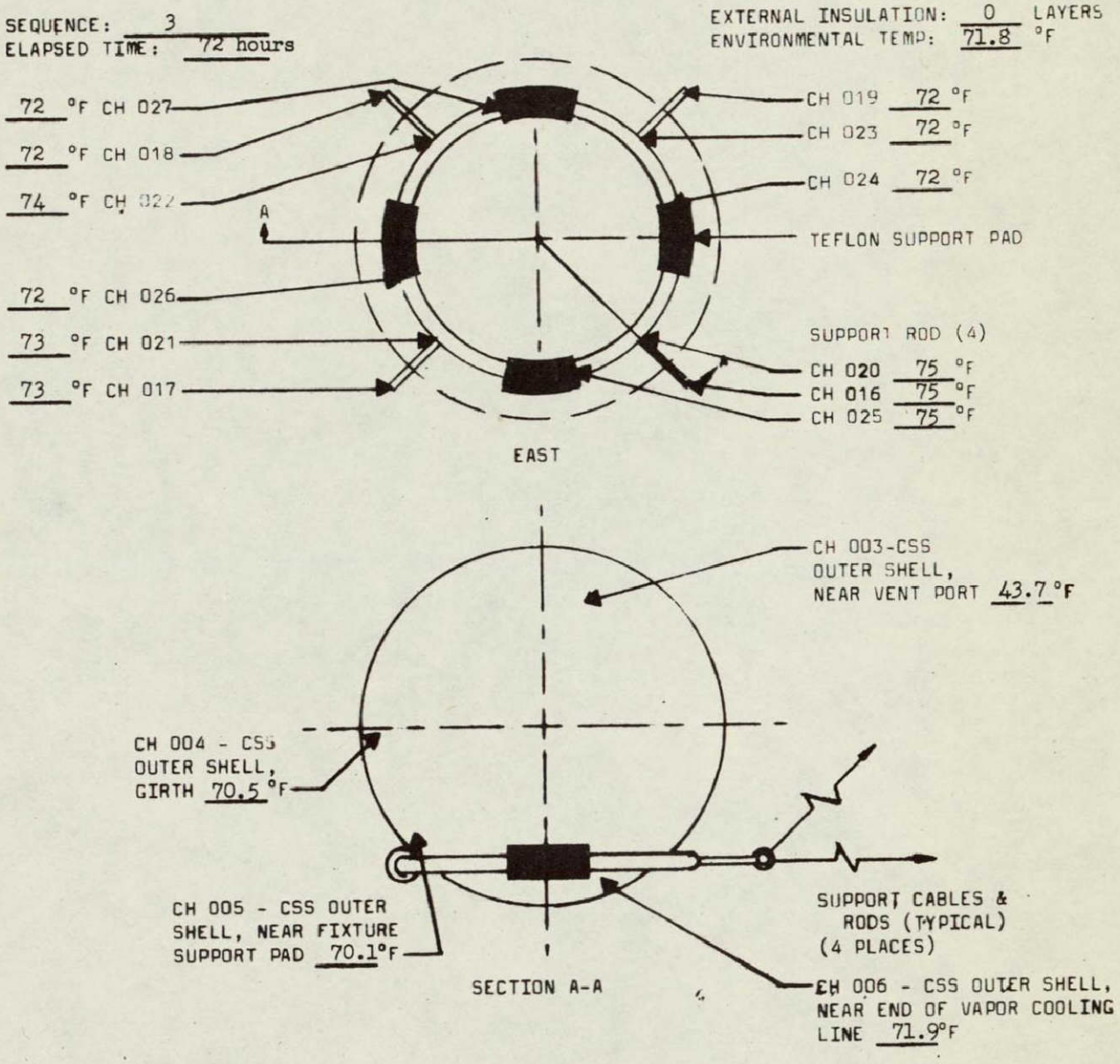

Average Temperature of Outer Shell (Channels 003, 004, 005, and 006) 64.0°F.

Sequence 3 final temperature plot.

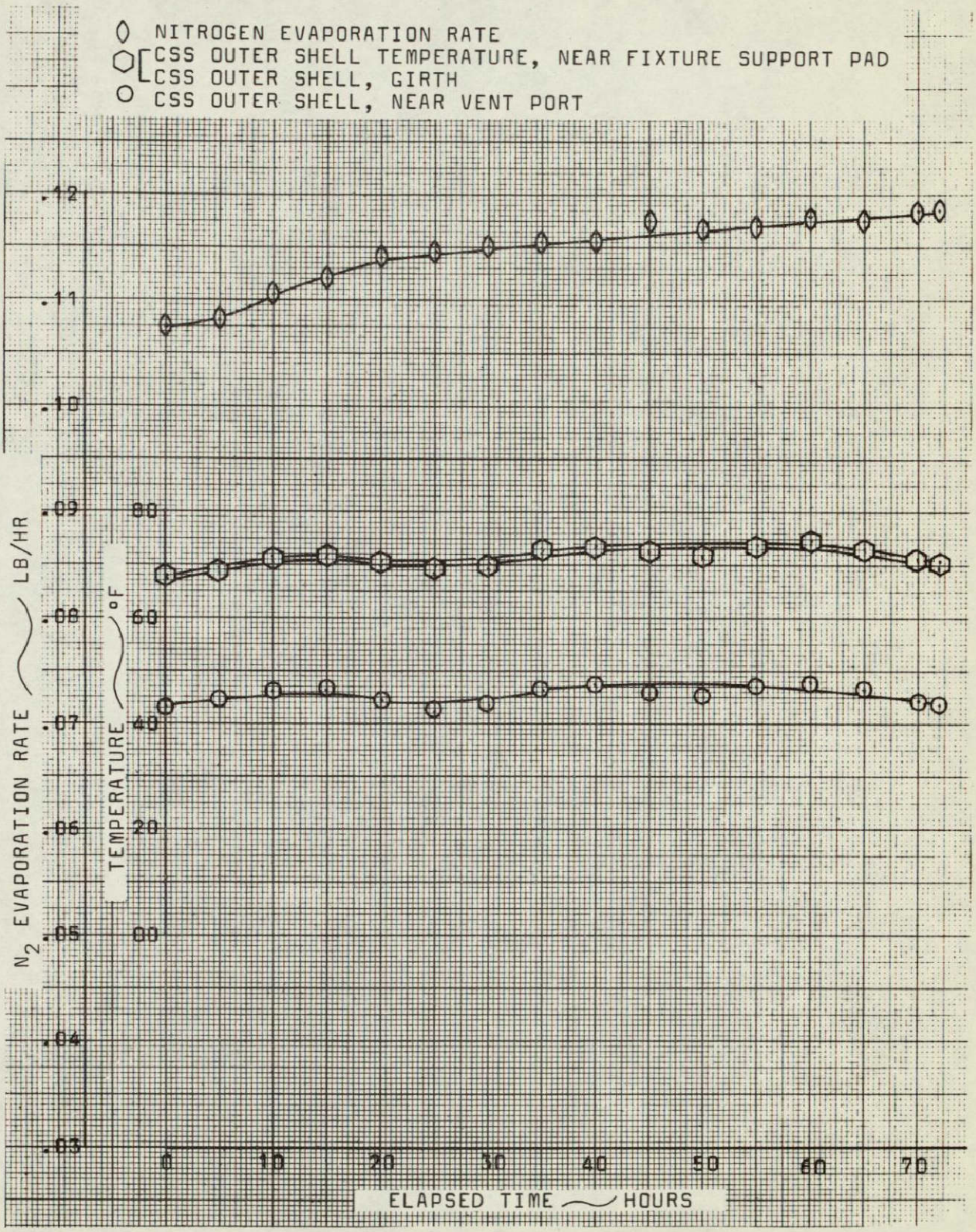

Sequence 3 CSS temperature and evaporation rate versus ET.

SEQUENCE: 4
ELAPSED TIME: 127 hours

EXTERNAL INSULATION: 50 LAYERS
ENVIRONMENTAL TEMP: 0.3 °F

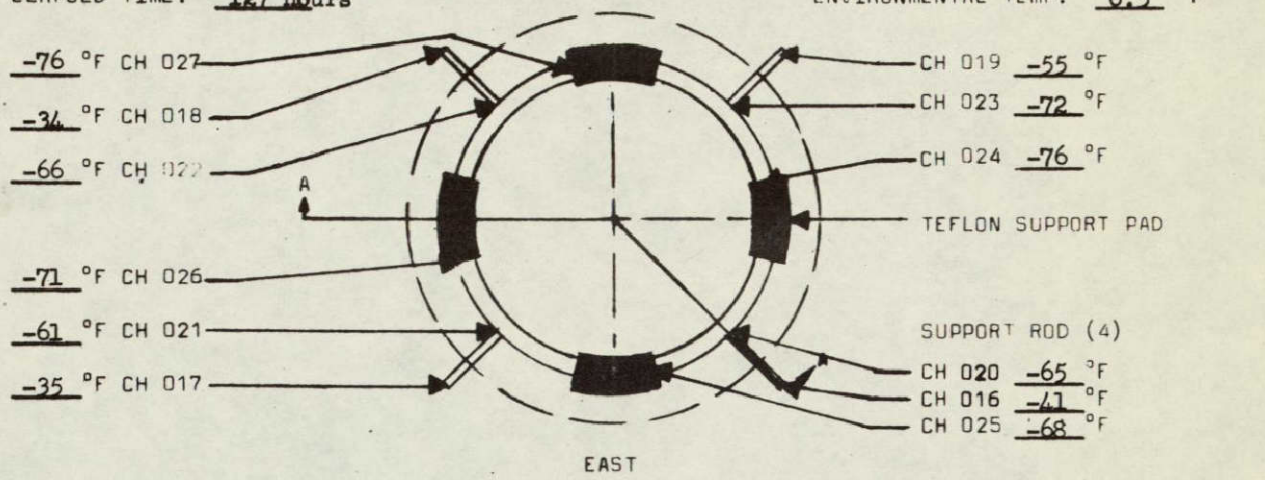

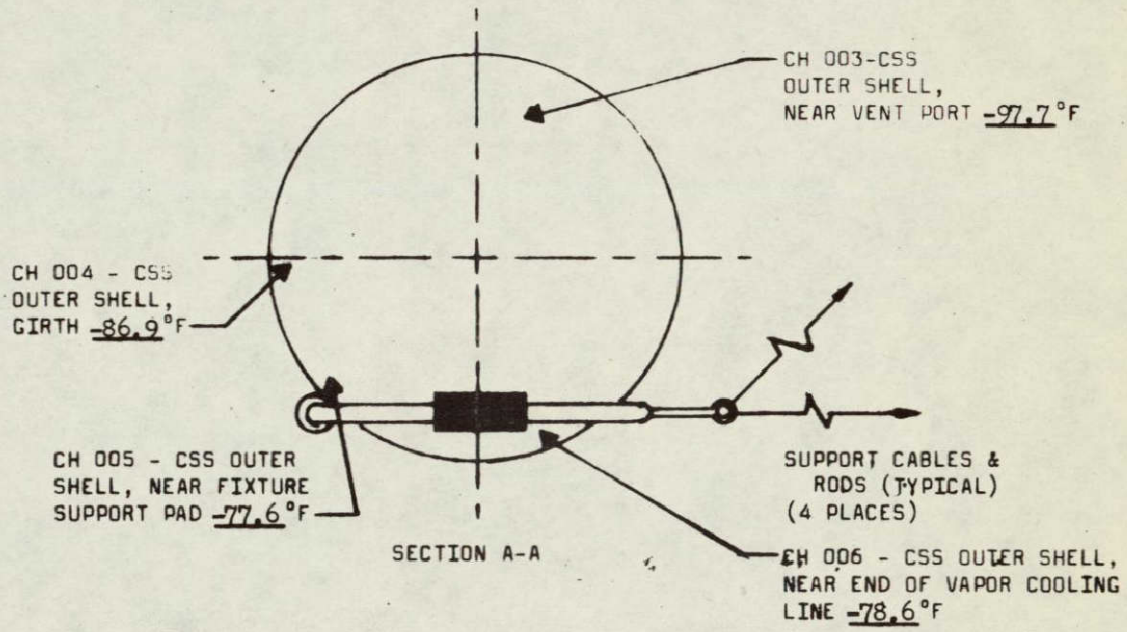

INSULATION TEMPERATURE GRADIENT

Average Temperature of Outer Shell (Channels 003, 004, 005, and 006) = -85.5 °F

Channel	Layer	Description	Temperature
008	24	External Insulation, Girth	-36.6 °F
009	36	External Insulation, Girth	-20.0 °F

Average Temperature of Exterior of External Insulation (Channels 010 and 012) = -1.1 °F

Sequence 4 final temperature plot.

DOC. NO. MSC-67-R-EP-15
REVISION New
PAGE A8 OF A26

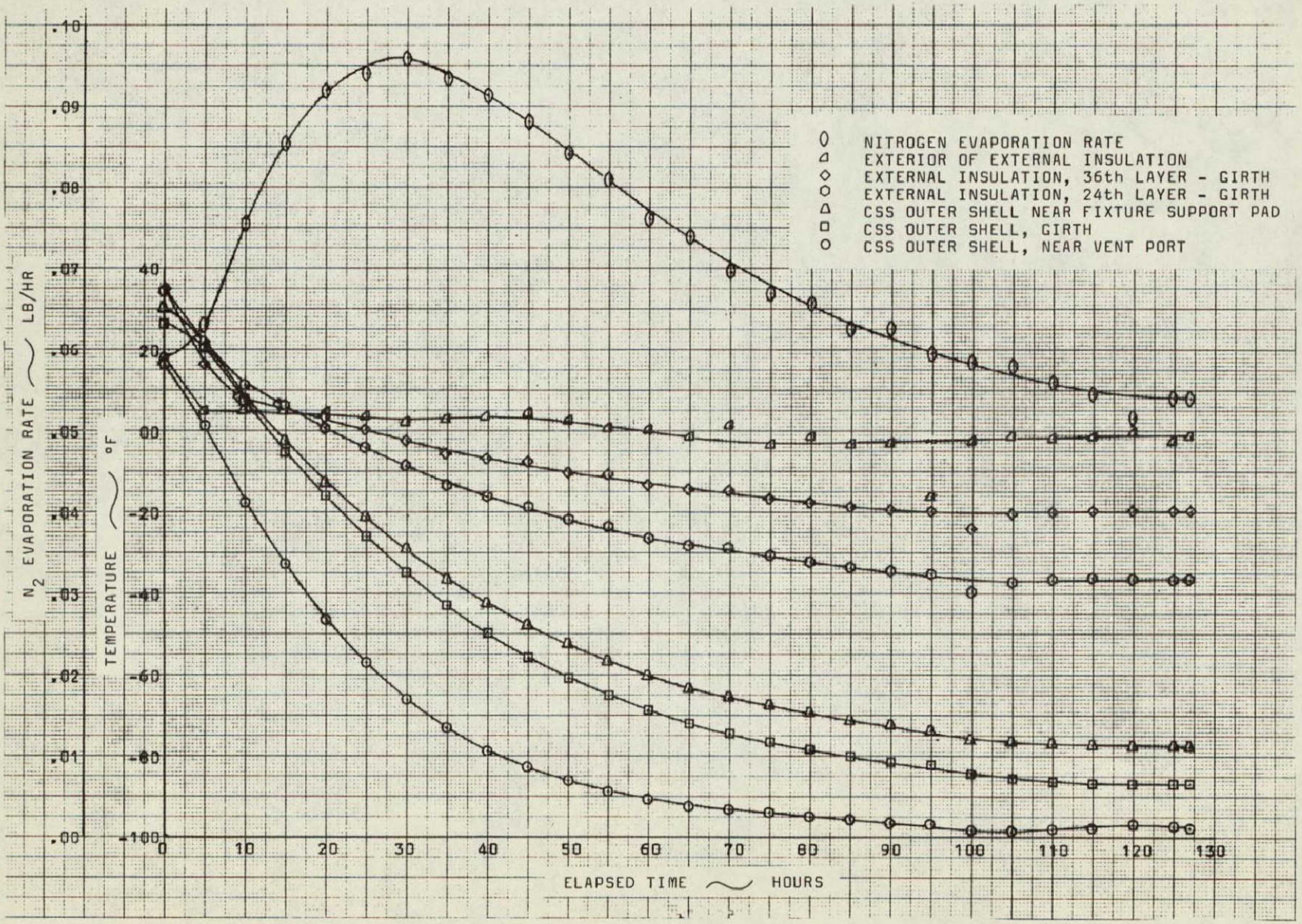

Sequence 4 CSS temperature and evaporation rate versus ET.

MSC FORM 360B (JAN 67)

SEQUENCE: 5
ELAPSED TIME: 130 hours

EXTERNAL INSULATION: 50 LAYERS
ENVIRONMENTAL TEMP: 69.9 °F

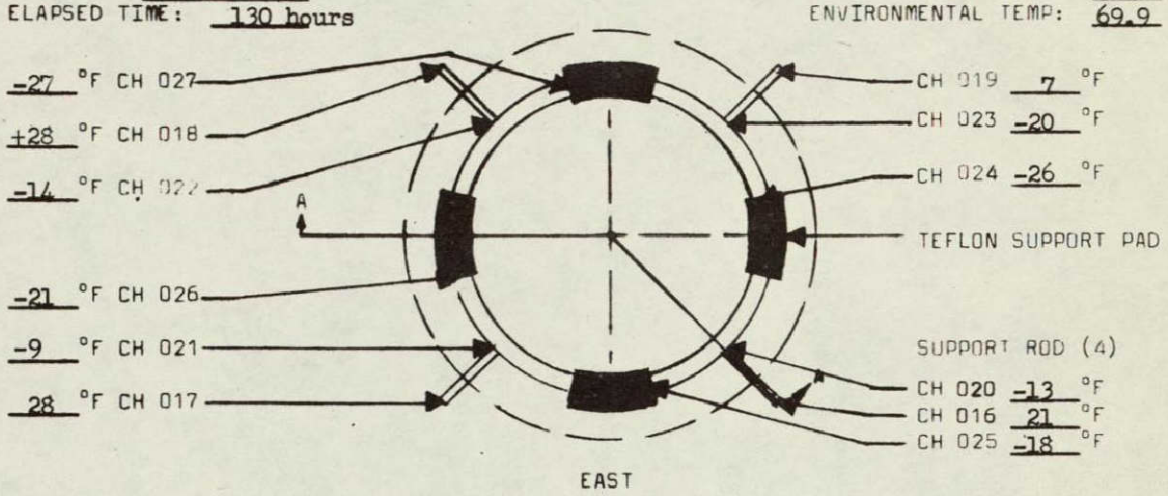

EAST

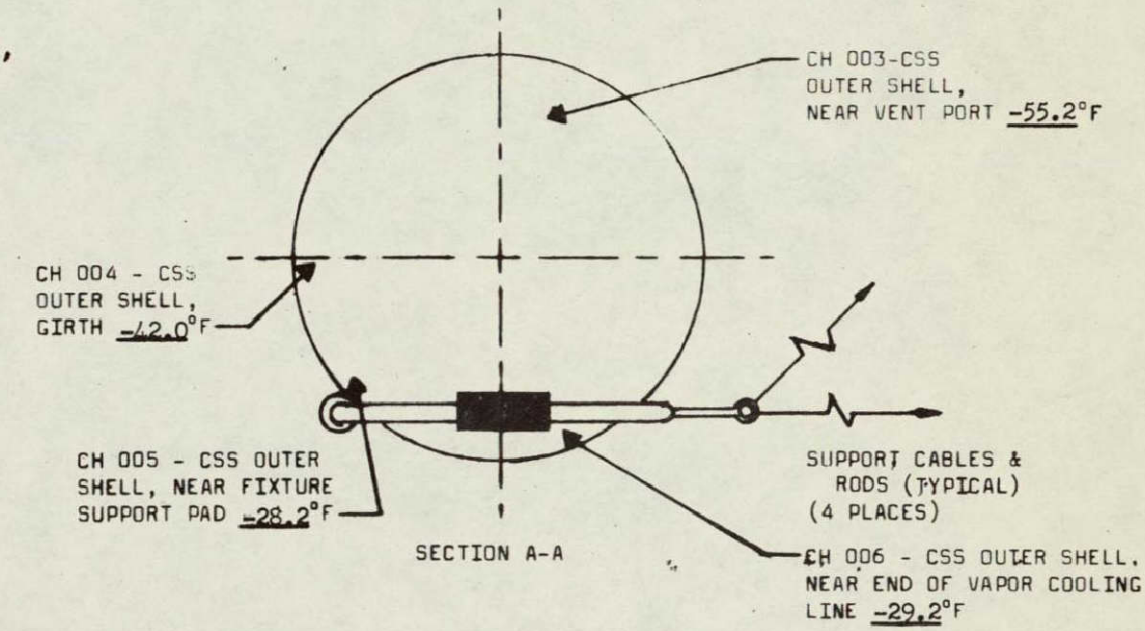

SECTION A-A

INSULATION TEMPERATURE GRADIENT

Average Temperature of Outer Shell (Channels 003, 004, 005, and 006) = -38.7 °F

Channel	Layer	Description	Temperature
008	24	External Insulation, Girth	21.2°F
009	36	External Insulation, Girth	43.4°F

Average Temperature of Exterior of External Insulation (Channels 010 and 012) = 66.7 °F

Sequence 5 final temperature plot.

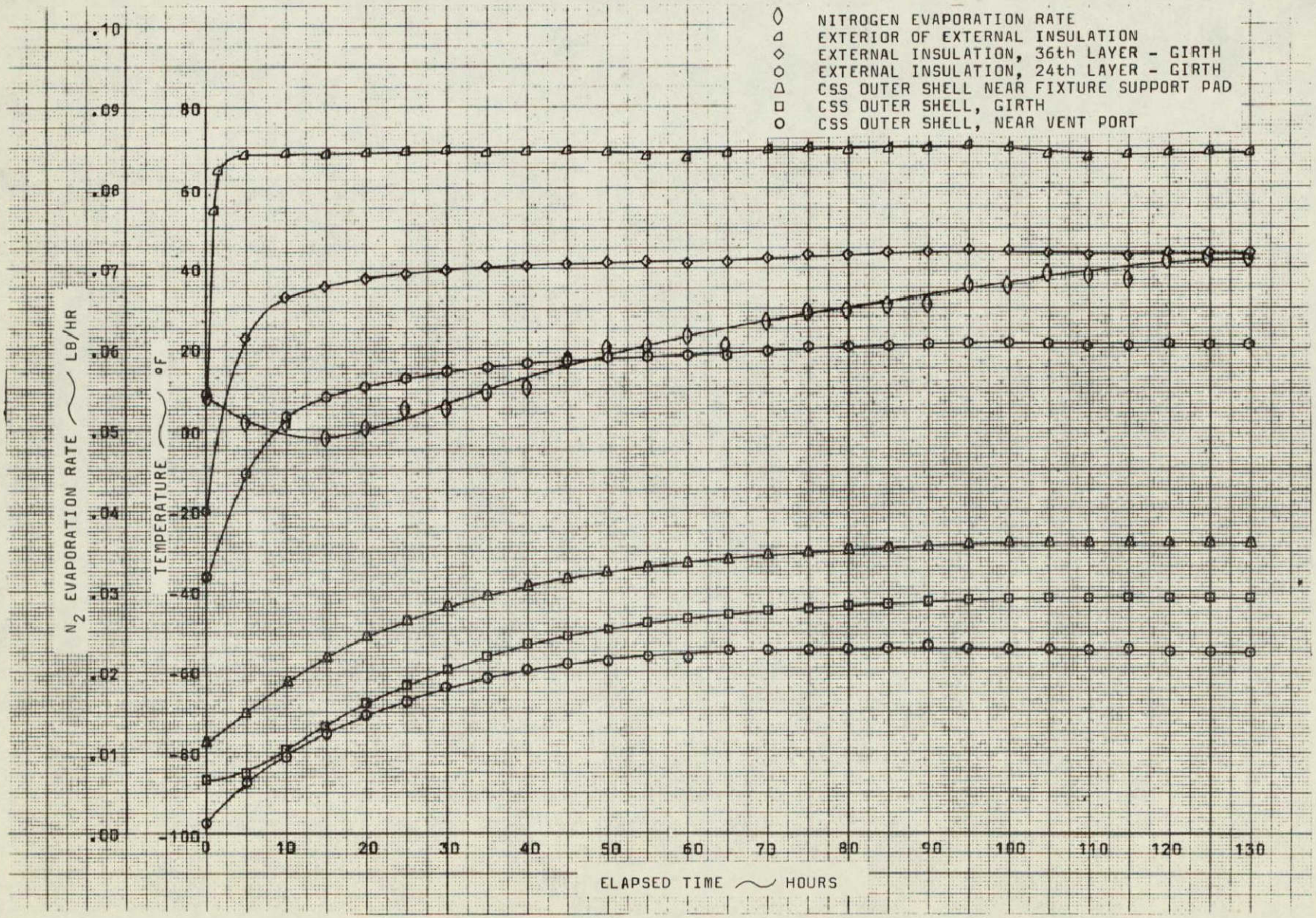

Sequence 5 CSS temperature and evaporation rate versus ET.

SEQUENCE: 6
ELAPSED TIME: 100 hours

EXTERNAL INSULATION: 50 LAYERS
ENVIRONMENTAL TEMP: 141.1 °F

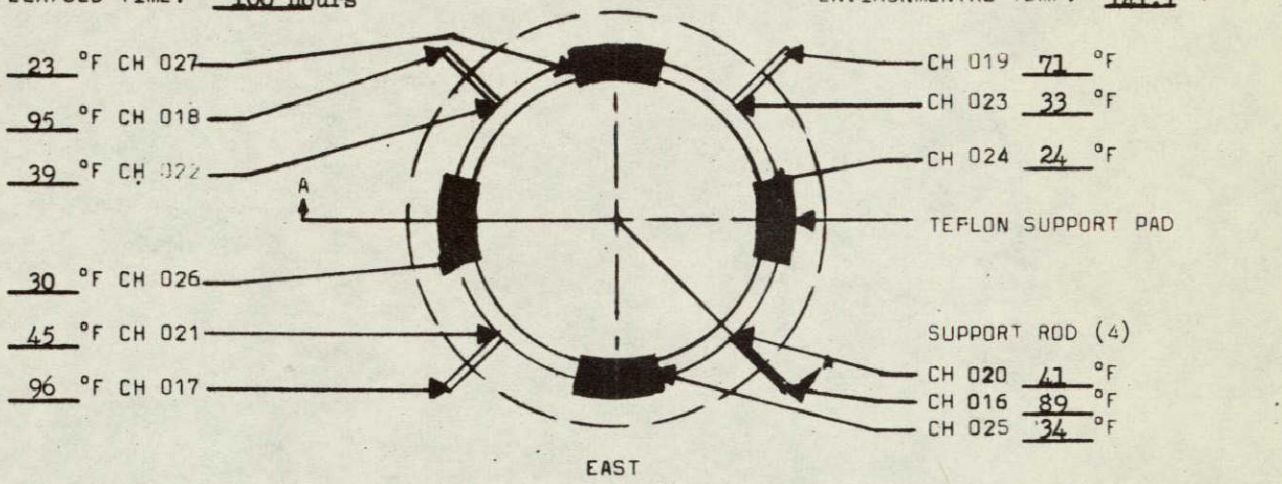

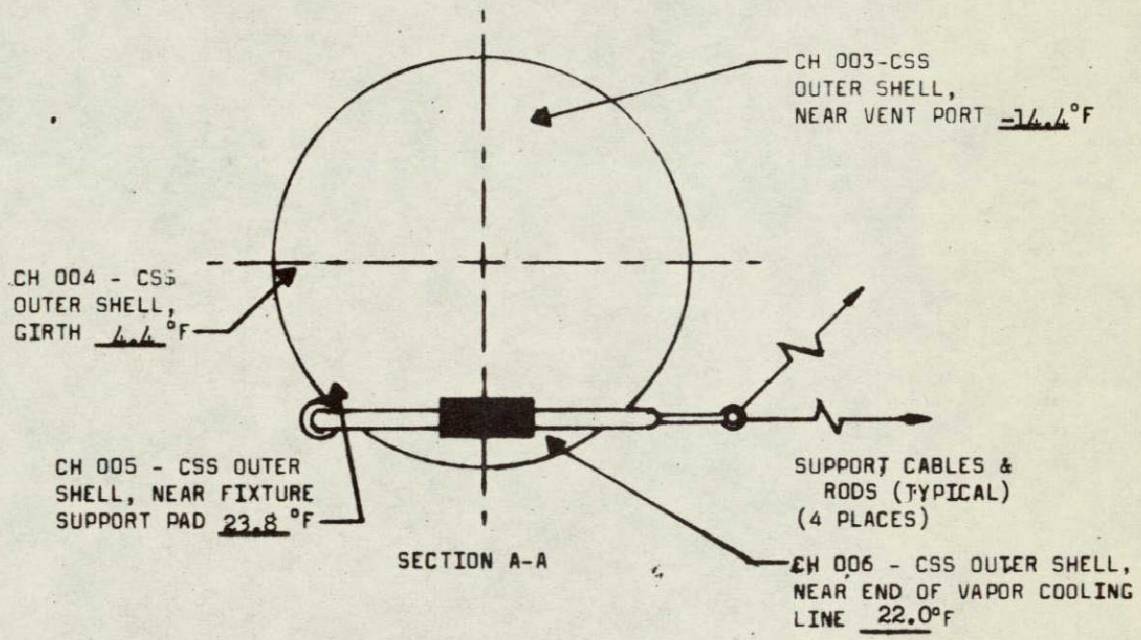

INSULATION TEMPERATURE GRADIENT

Average Temperature of Outer Shell (Channels 003, 004, 005, and 006) = 8.4°F

Channel	Layer	Description	Temperature
008	24	External Insulation, Girth	80.0°F
009	36	External Insulation, Girth	109.8°F

Average Temperature of Exterior of External Insulation (Channels 010 and 012) = 139.8°F

Sequence 6 final temperature plot.

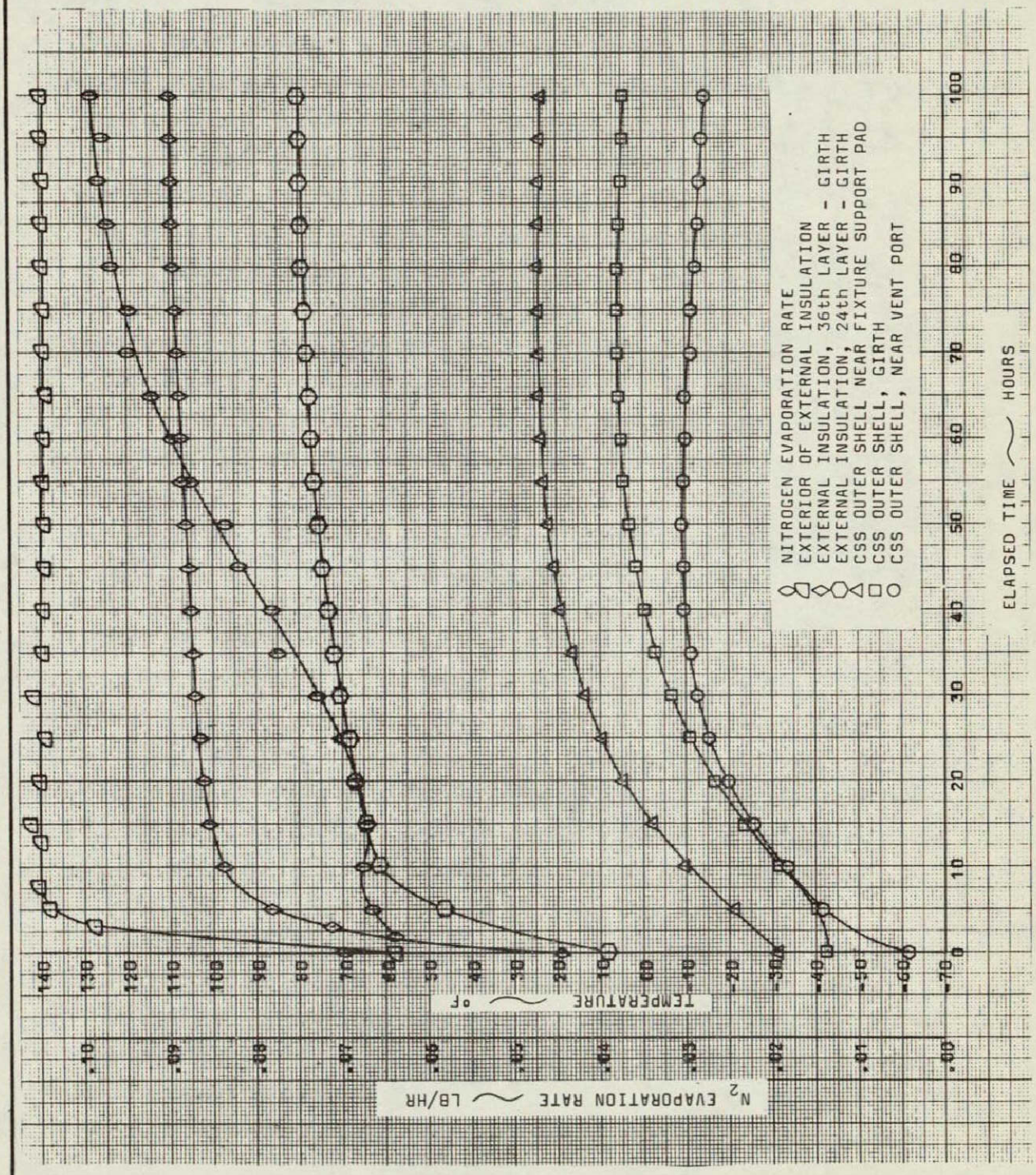

Sequence 6 CSS temperature and evaporation rate versus ET.

SEQUENCE: 7
ELAPSED TIME: 206 hours

EXTERNAL INSULATION: 100 LAYERS
ENVIRONMENTAL TEMP: 1.1 °F

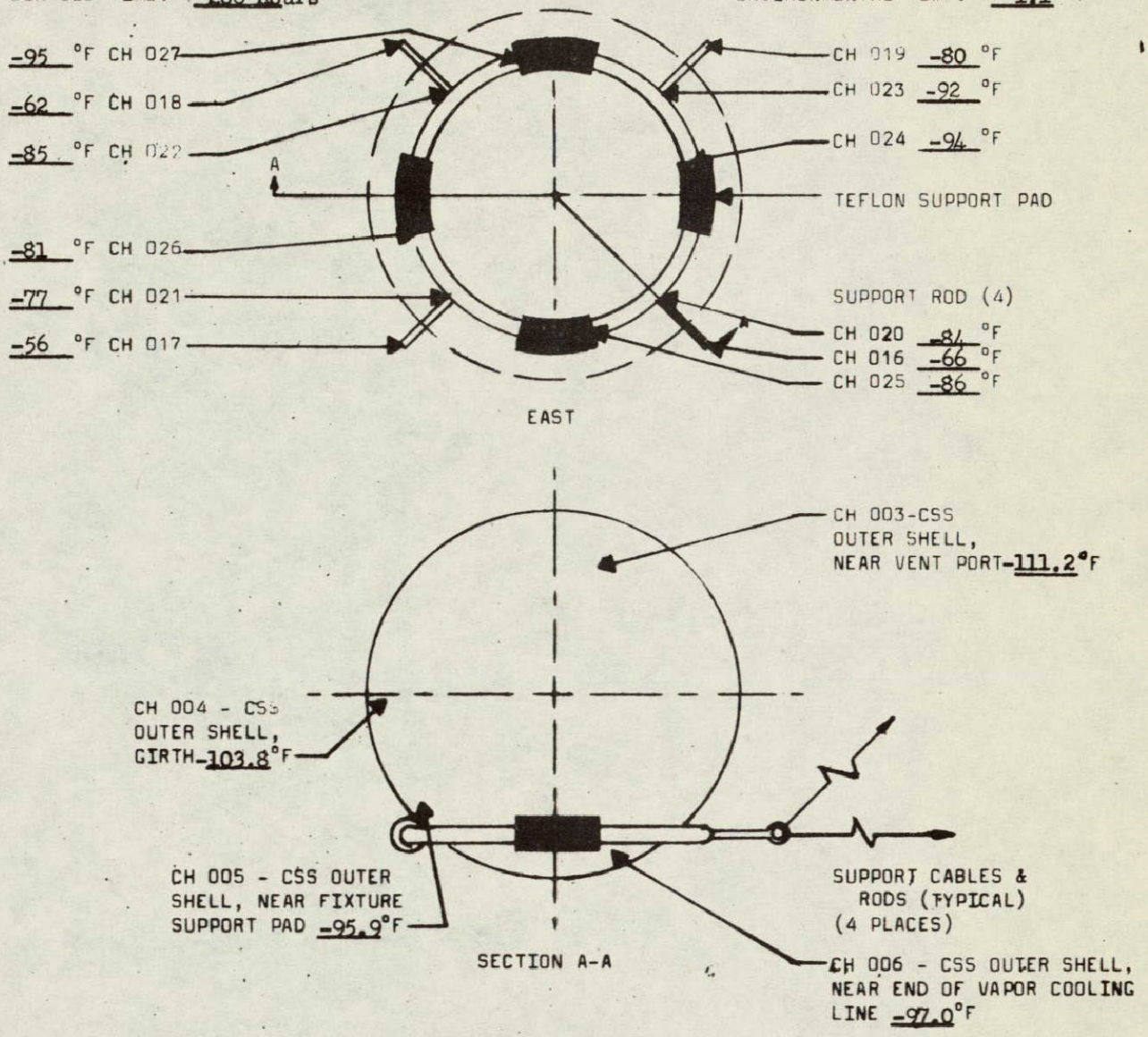

INSULATION TEMPERATURE GRADIENT

Average Temperature of Outer Shell (Channels 003, 004, 005 and 006) = -102.0°F

Channel	Layer	Description	Temperature
007	12	External Insulation, Girth	-70.0°F
008	24	External Insulation, Girth	-52.9 °F
009	36	External Insulation, Girth	-45.2°F
010	75	Exterior of External Insulation, Girth	-18.0°F

Average Temperature of Exterior of External Insulation (Channels 011 and 012) = 4.6°F

Sequence 7 final temperature plot.

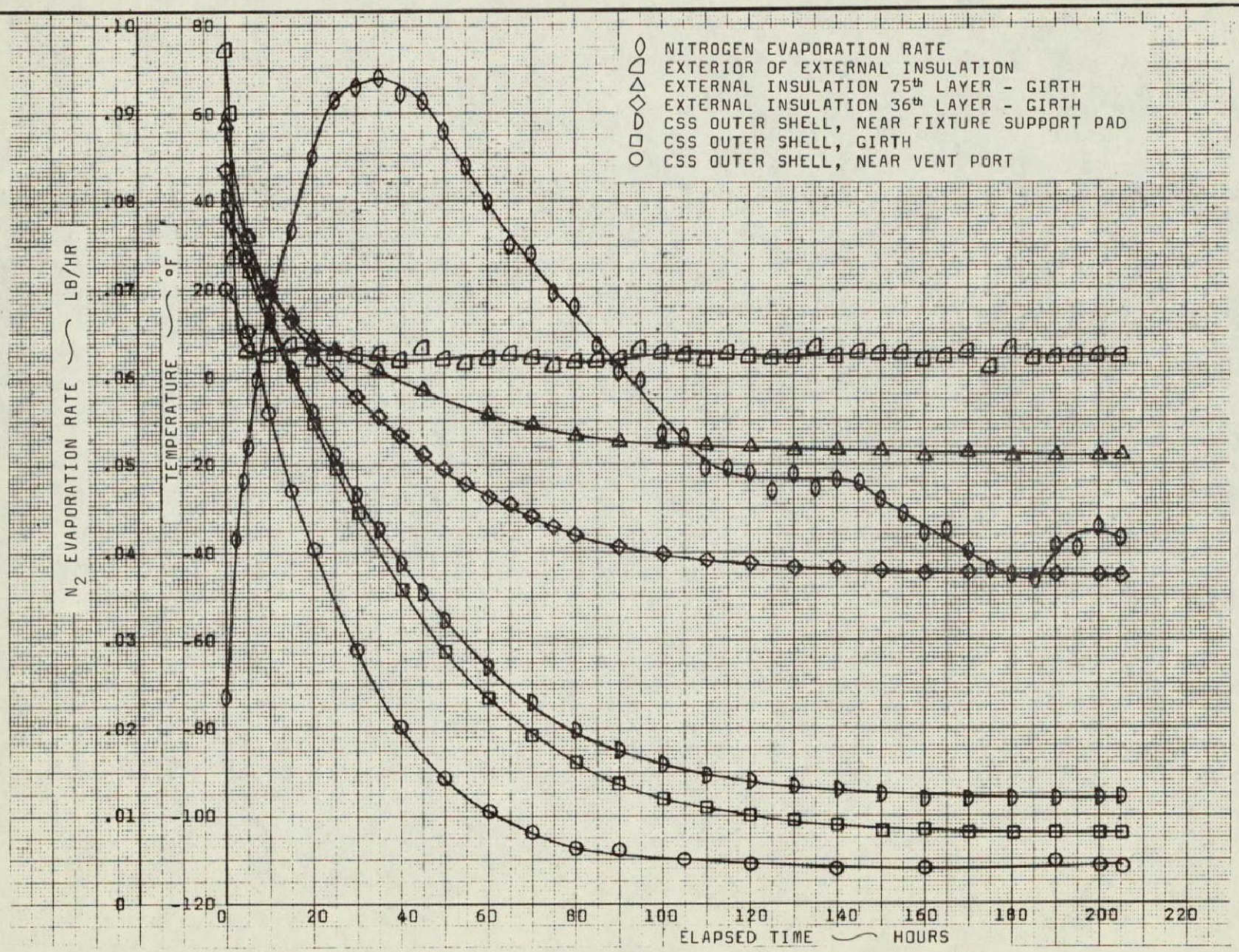

Sequence 7 CSS temperature and evaporation rate versus ET.

SEQUENCE: 8
ELAPSED TIME: 160 hours

EXTERNAL INSULATION: 100 LAYERS
ENVIRONMENTAL TEMP: 67.1 °F

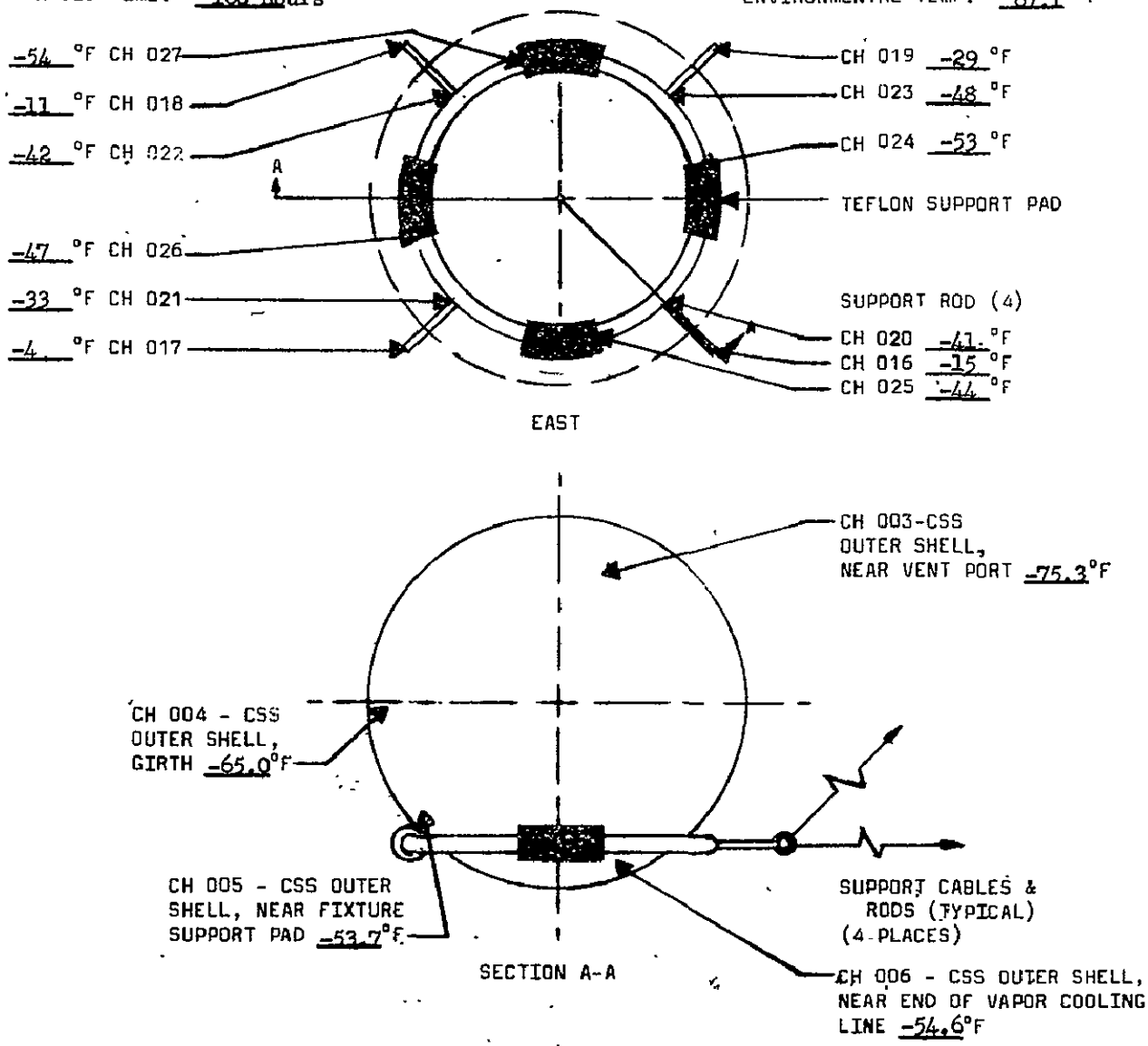

INSULATION TEMPERATURE GRADIENT

Average Temperature of Outer Shell (Channels 003, 004, 005, and 006) = -62.2°F

Channel	Layer	Description	Temperature
007	12	External Insulation, Girth	-24.5°F
008	24	External Insulation, Girth	-3.6°F
009	36	External Insulation, Girth	6.5°F
010	75	Exterior of External Insulation, Girth	40.5°F

Average Temperature of Exterior of External Insulation (Channels 011 and 012) = 67.5°F

Sequence 8 final temperature plot.

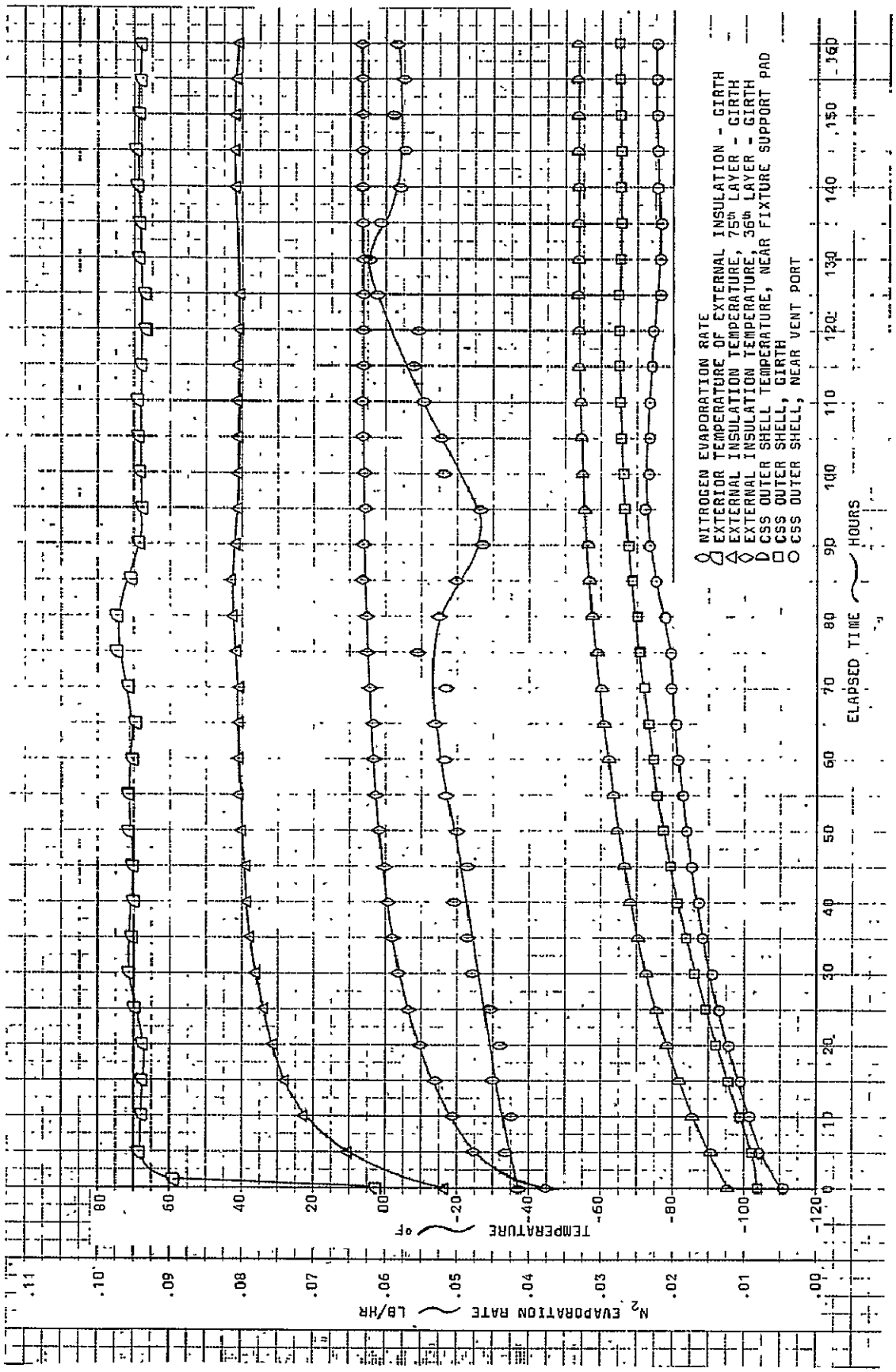

Sequence 8 CSS temperature and evaporation rate versus ET.

SEQUENCE: 9
ELAPSED TIME: 72 hours

EXTERNAL INSULATION: 25 LAYERS
ENVIRONMENTAL TEMP: -74.1 °F

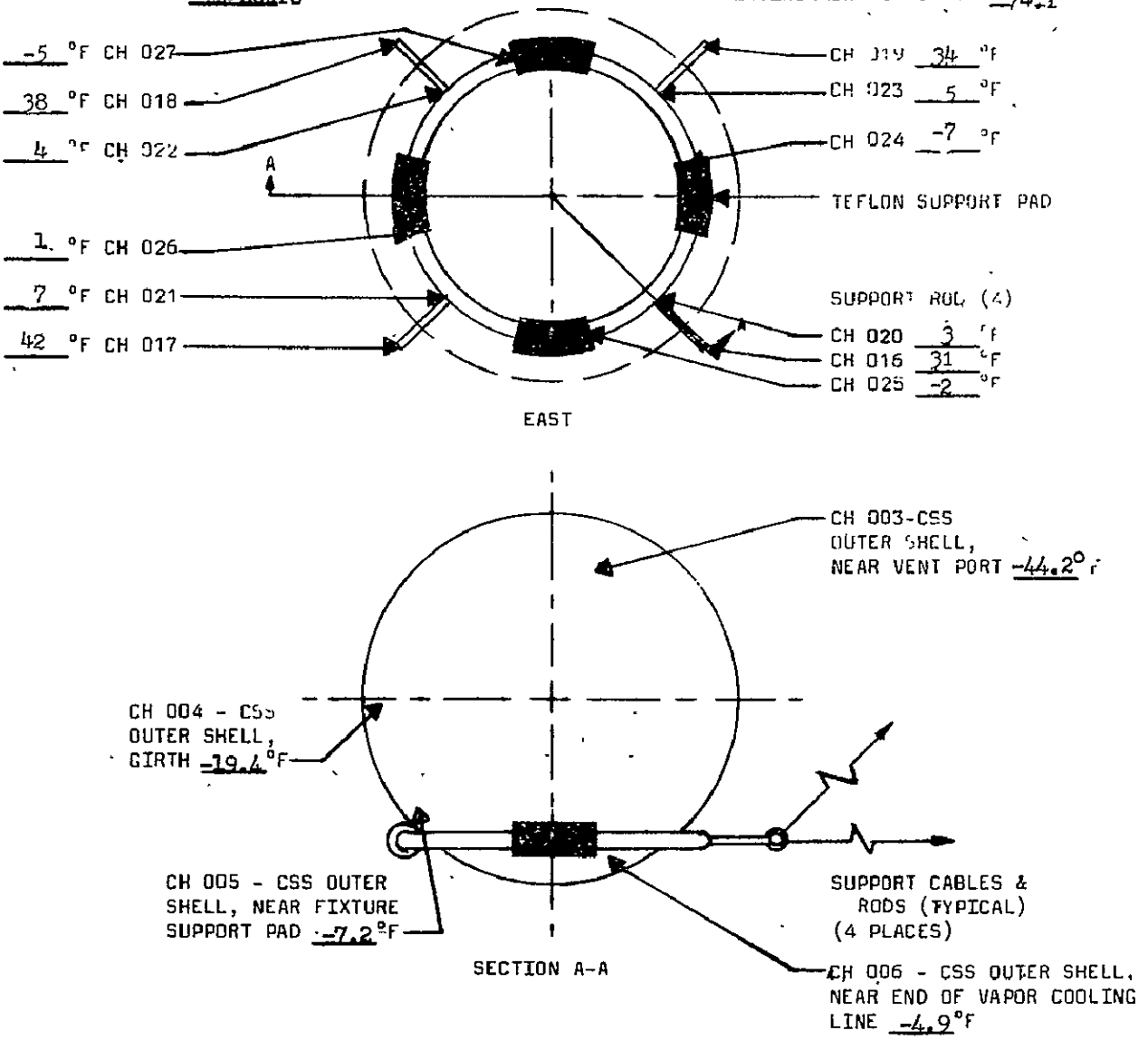

INSULATION TEMPERATURE GRADIENT

Average Temperature of Outer Shell (Channels 003, 004, 005, and 006) = 18.9°F

Channel	Layer	Description	Temperature
007	6	External Insulation, Girth	11.7°F
008	12	External Insulation, Girth	38.5°F
009	18	External Insulation, Girth	50.5°F

Average Temperature of Exterior of External Insulation (Channels 010, 011, and 012) = 74.6°F

Sequence 9 final temperature plot.

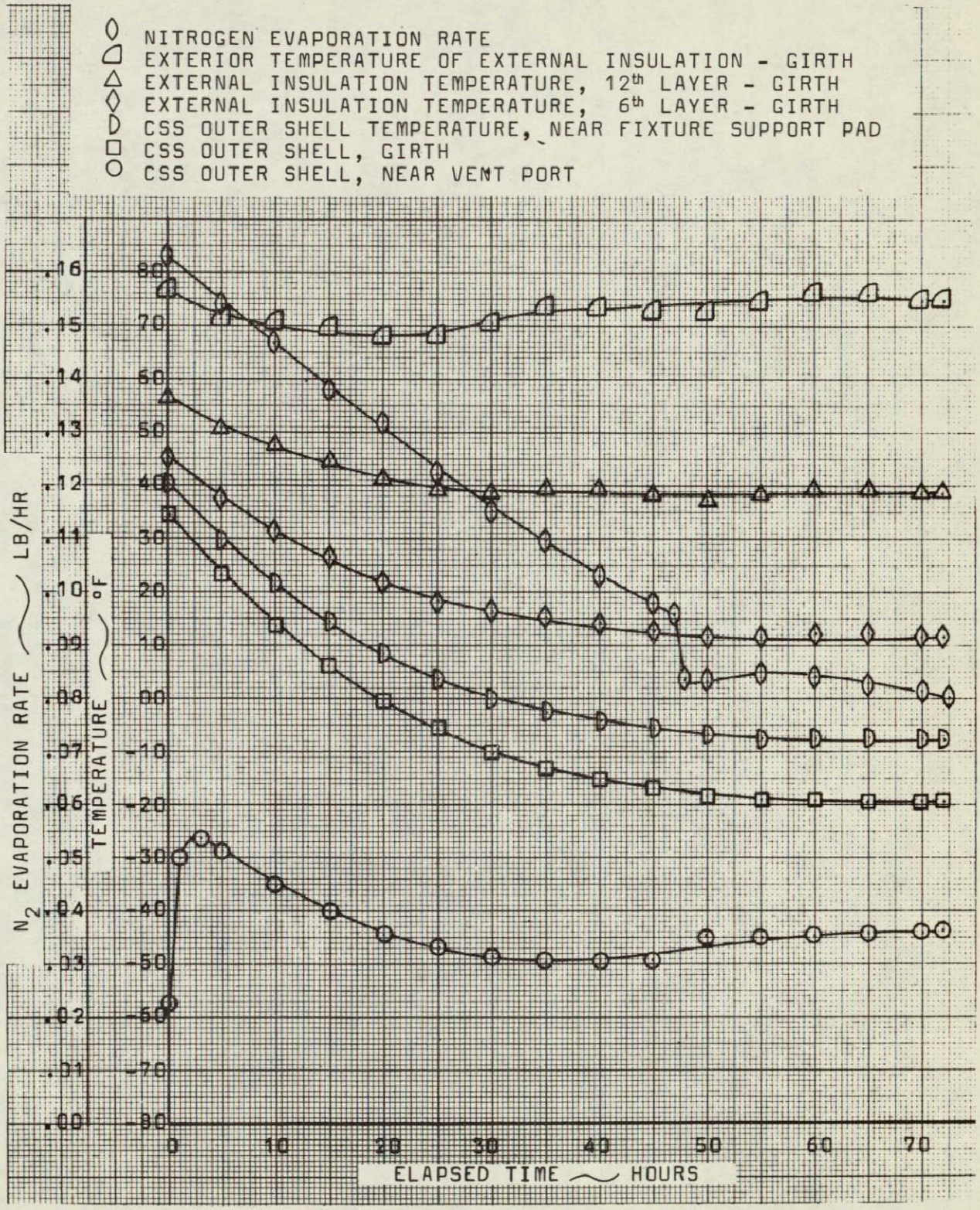

Sequence 9 CSS temperature and evaporation rate versus ET.

SEQUENCE: 10
ELAPSED TIME: 91 hours

EXTERNAL INSULATION: 25 LAYERS
ENVIRONMENTAL TEMP: -0.8 °F

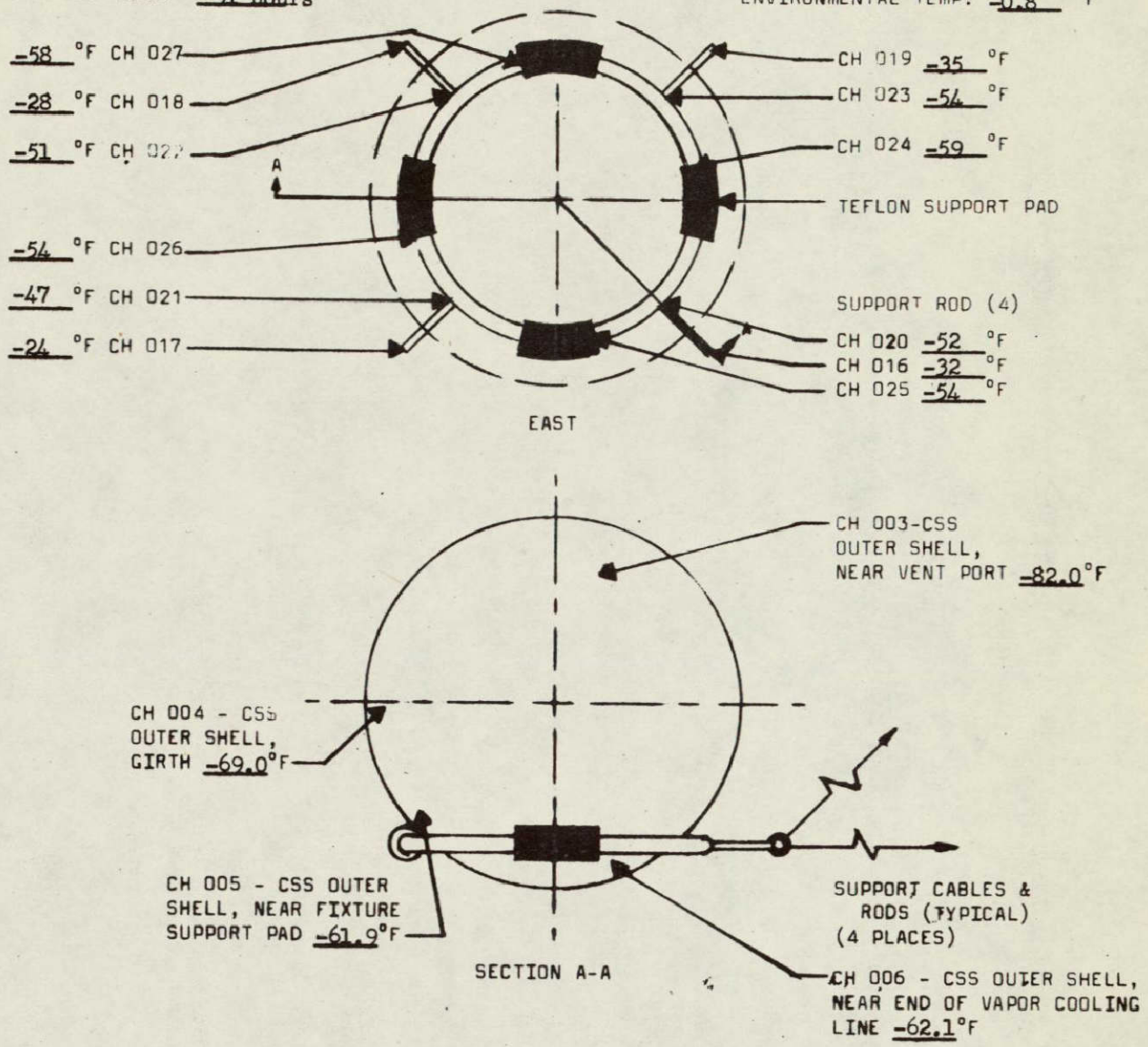

INSULATION TEMPERATURE GRADIENT

Average Temperature of Outer Shell (Channels 003, 004, 005, and 006) = -68.7°F

Channel	Layer	Description	Temperature
007	6	External Insulation, Girth	-45.4°F
008	12	External Insulation, Girth	-25.3°F
009	18	External Insulation, Girth	-16.9°F

Average Temperature of Exterior of External Insulation (Channels 010, 011, and 012) = 3.2°F

Sequence 10 final temperature plot.

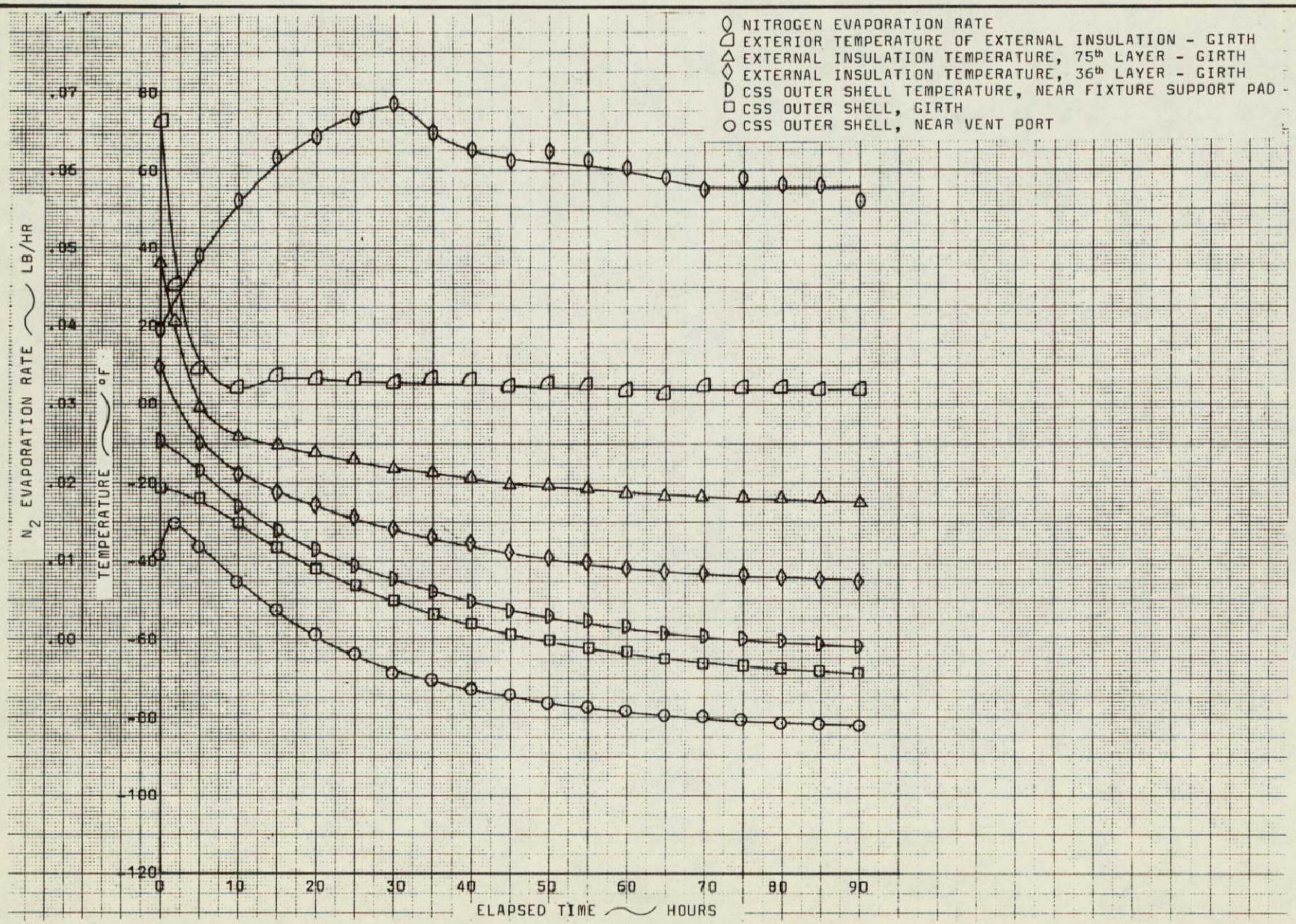

Sequence 10 CSS temperature and evaporation rate versus ET.

SEQUENCE: 11
ELAPSED TIME: 75 hours

EXTERNAL INSULATION: 25 LAYER
ENVIRONMENTAL TEMP: 72.9 °F

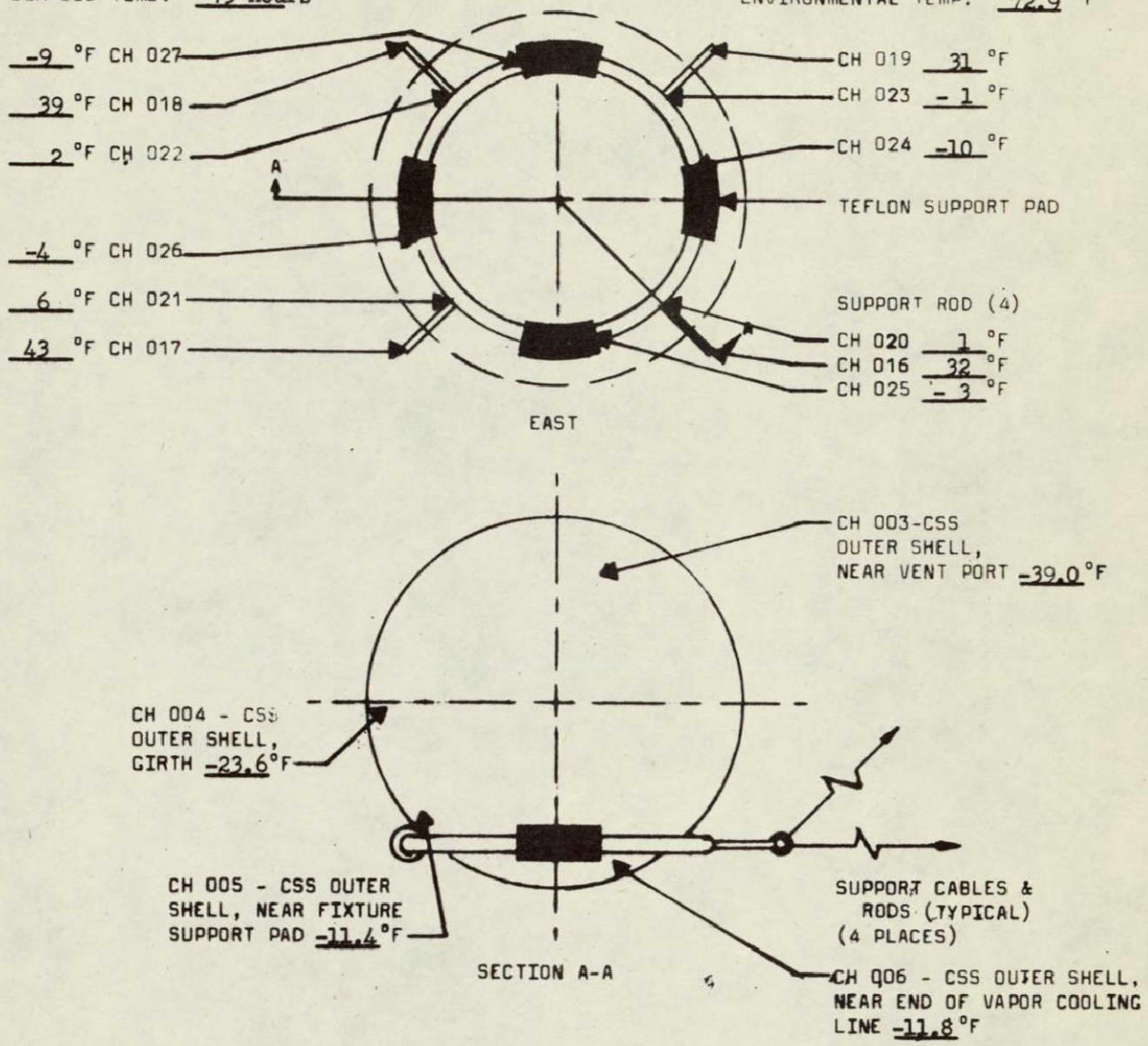

INSULATION TEMPERATURE GRADIENT

Average Temperature of Outer Shell (Channels 003, 004, 005, and 006) = -21.5°F

Channel	Layer	Description	Temperature
007	6	External Insulation, Girth	8.4°F
008	12	External Insulation, Girth	36.0°F
009	18	External Insulation, Girth	48.3°F

Average Temperature of Exterior of External Insulation (Channels 010, 011, and 012) = 73.6°F

Sequence 11 final temperature plot.

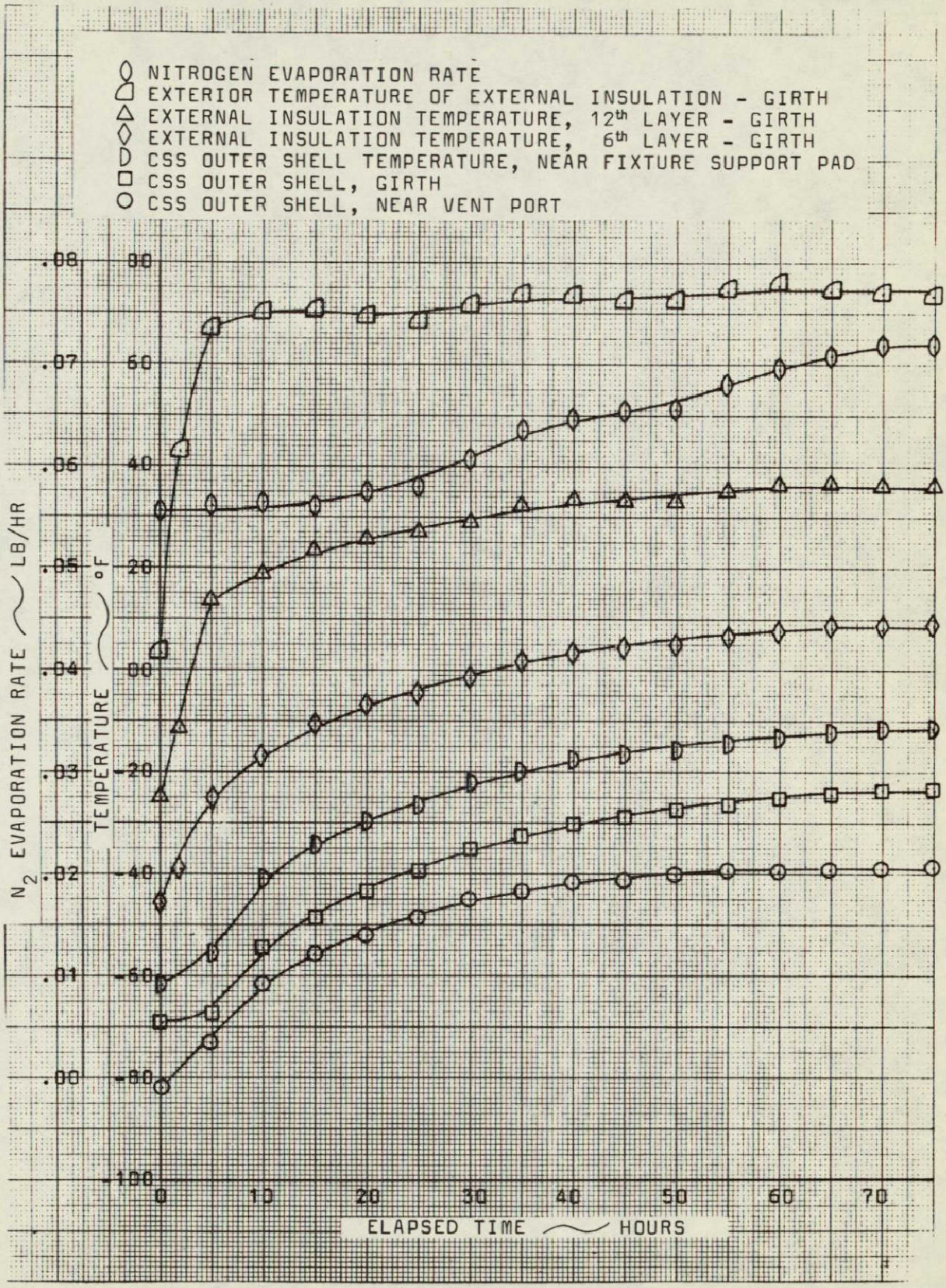

Sequence 11 CSS temperature and evaporation rate versus ET.

SEQUENCE: 12
ELAPSED TIME: 96 hours

EXTERNAL INSULATION: 25 LAYERS
ENVIRONMENTAL TEMP: 141 °F

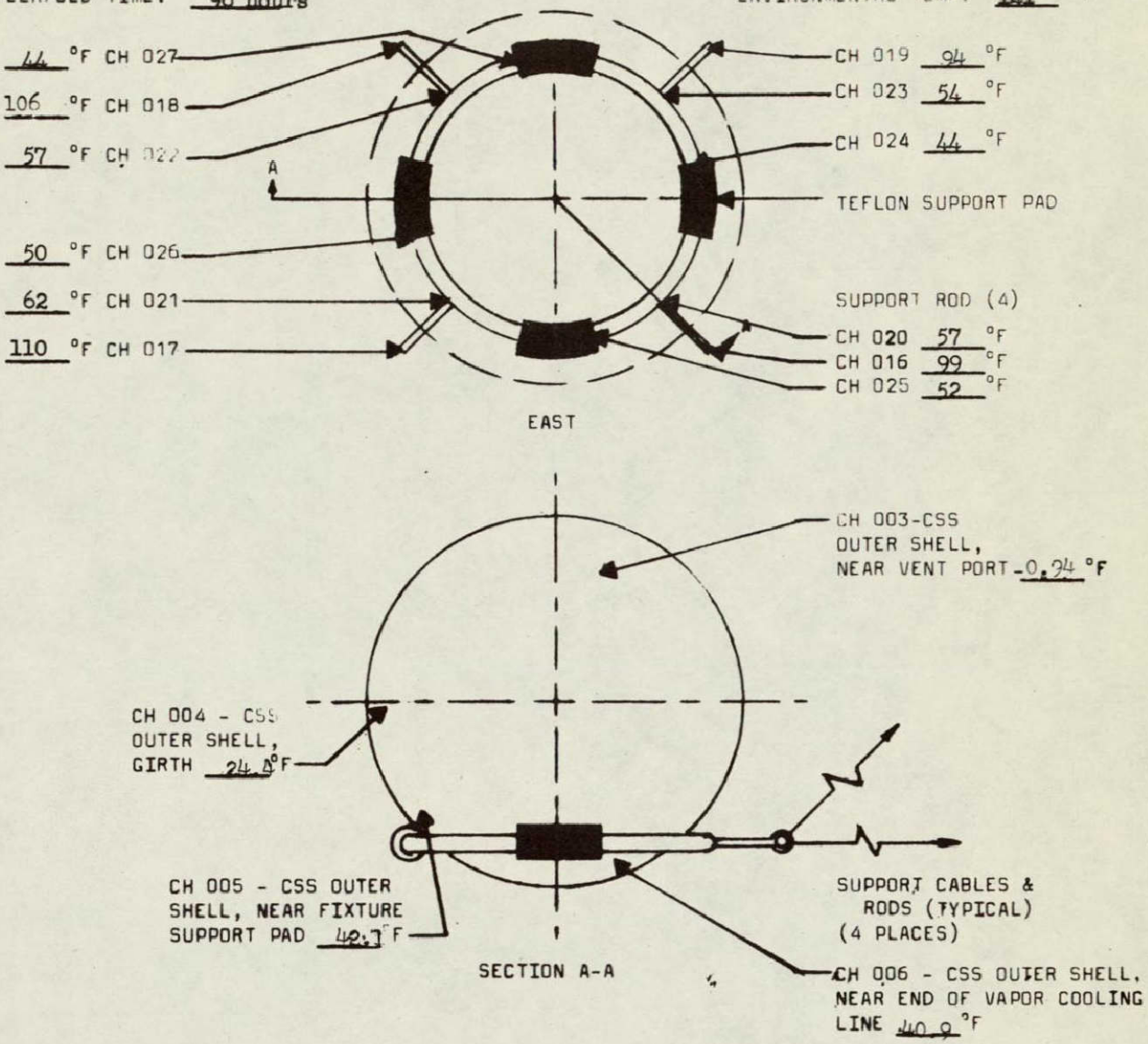

INSULATION TEMPERATURE GRADIENT

Average Temperature of Outer Shell (Channels 003, 004, 005, and 006) = 26.2°F

Channel	Layer	Description	Temperature
007	6	External Insulation, Girth	61.6°F
008	12	External Insulation, Girth	97.2°F
009	18	External Insulation, Girth	113.8°F

Average Temperature of Exterior of External Insulation (Channels 010, 011, and 012) = 144.2°F

Sequence 12 final temperature plot.

DOC. NO. MSC-67-R-EP-15
REVISION New
PAGE A24 OF A26

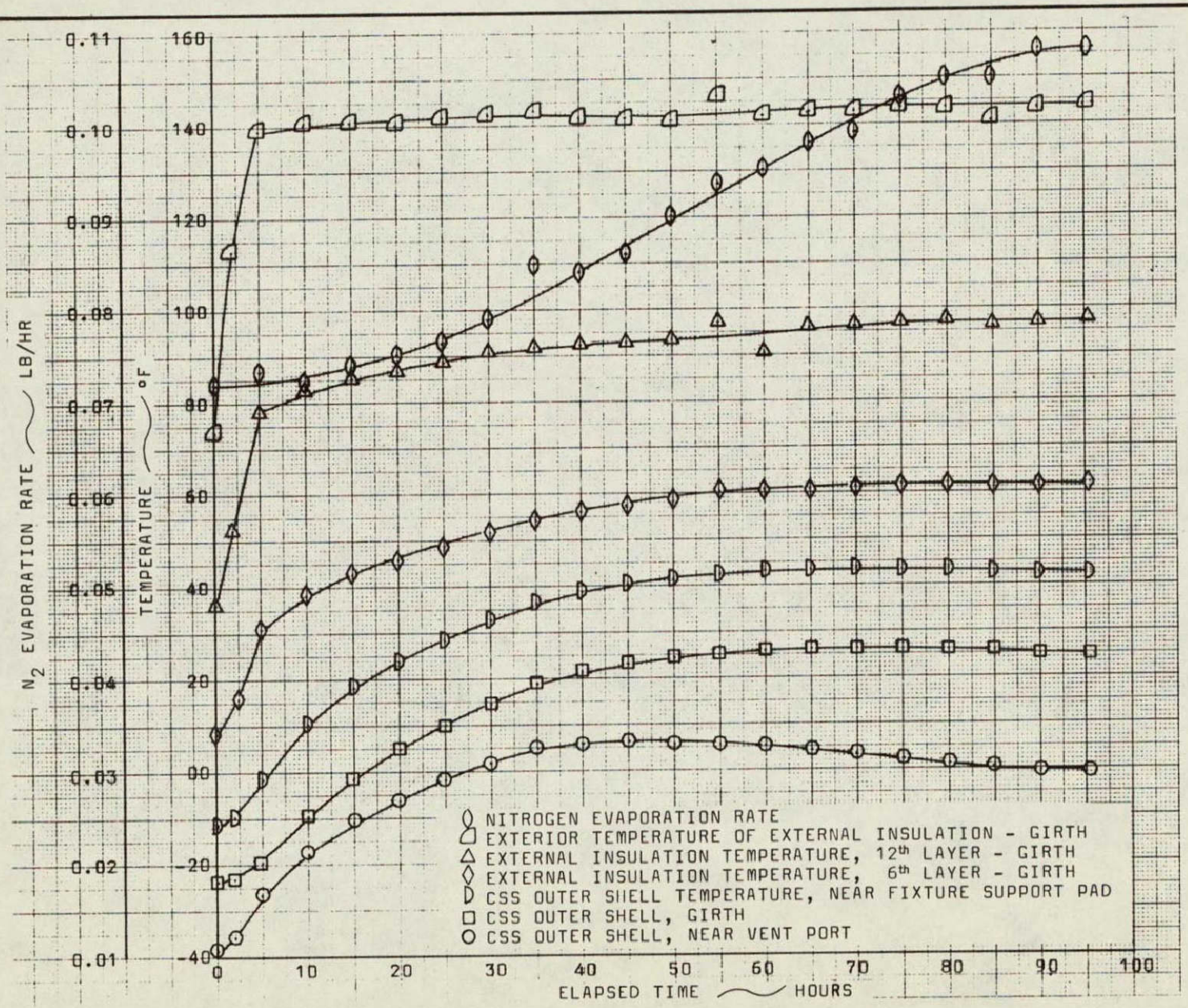

Sequence 12 CSS temperature and evaporation rate versus ET.

MSC FORM 360B (JAN 67)

SEQUENCE: 13
ELAPSED TIME: 86 hours

EXTERNAL INSULATION: 5 LAYERS
ENVIRONMENTAL TEMP: 73.5 °F

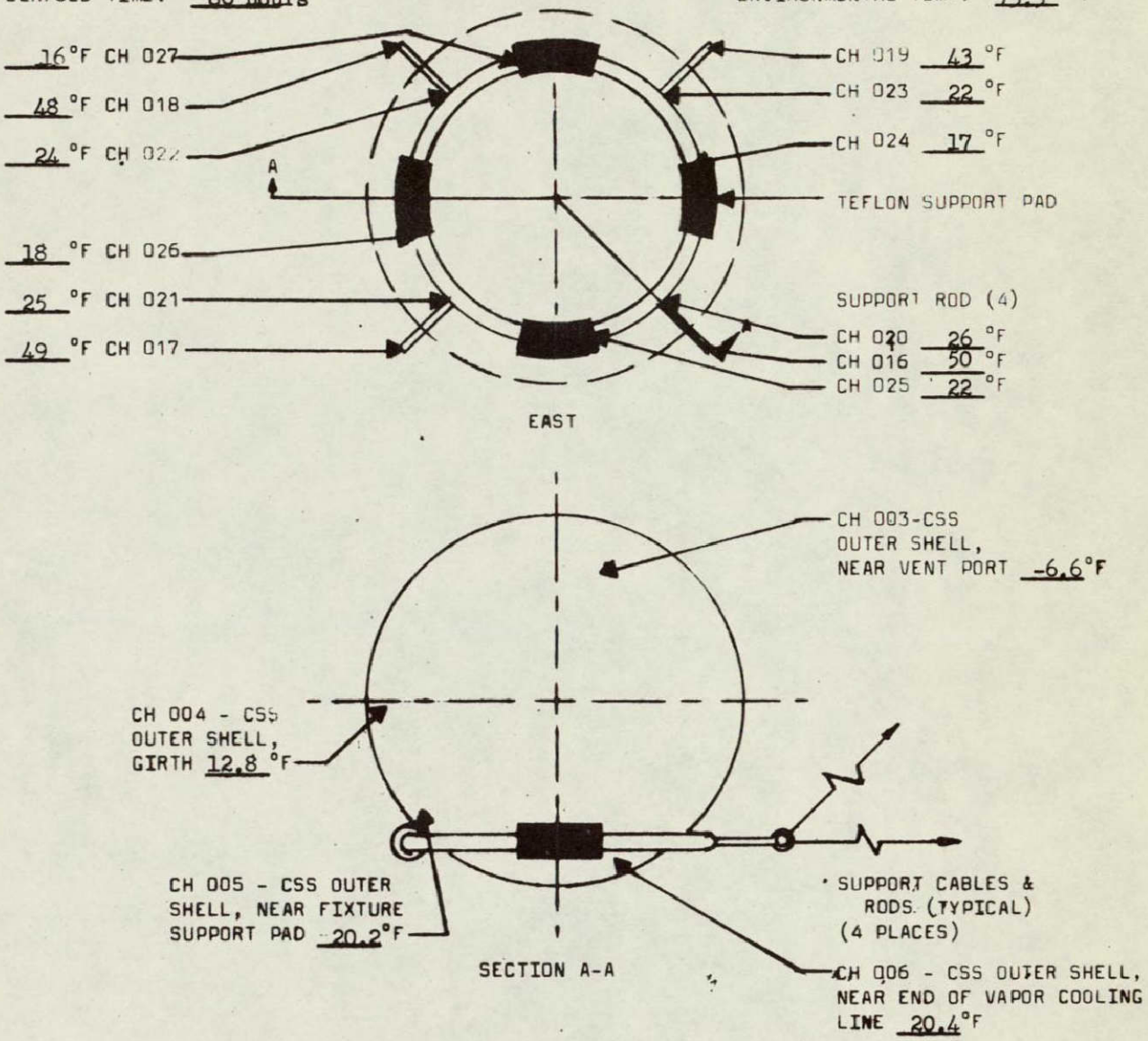

INSULATION TEMPERATURE GRADIENT

Average Temperature of Outer Shell (Channels 003, 004, 005, and 006) = 11.7°F

Channel	Layer	Description	Temperature
007	2	External Insulation, Girth	41.0°F
008	3	External Insulation, Girth	48.0°F
009	4	External Insulation, Girth	55.1°F

Average Temperature of Exterior of External Insulation (Channels 010, 011, and 012) = 72.2°F

Sequence 13 final temperature plot.

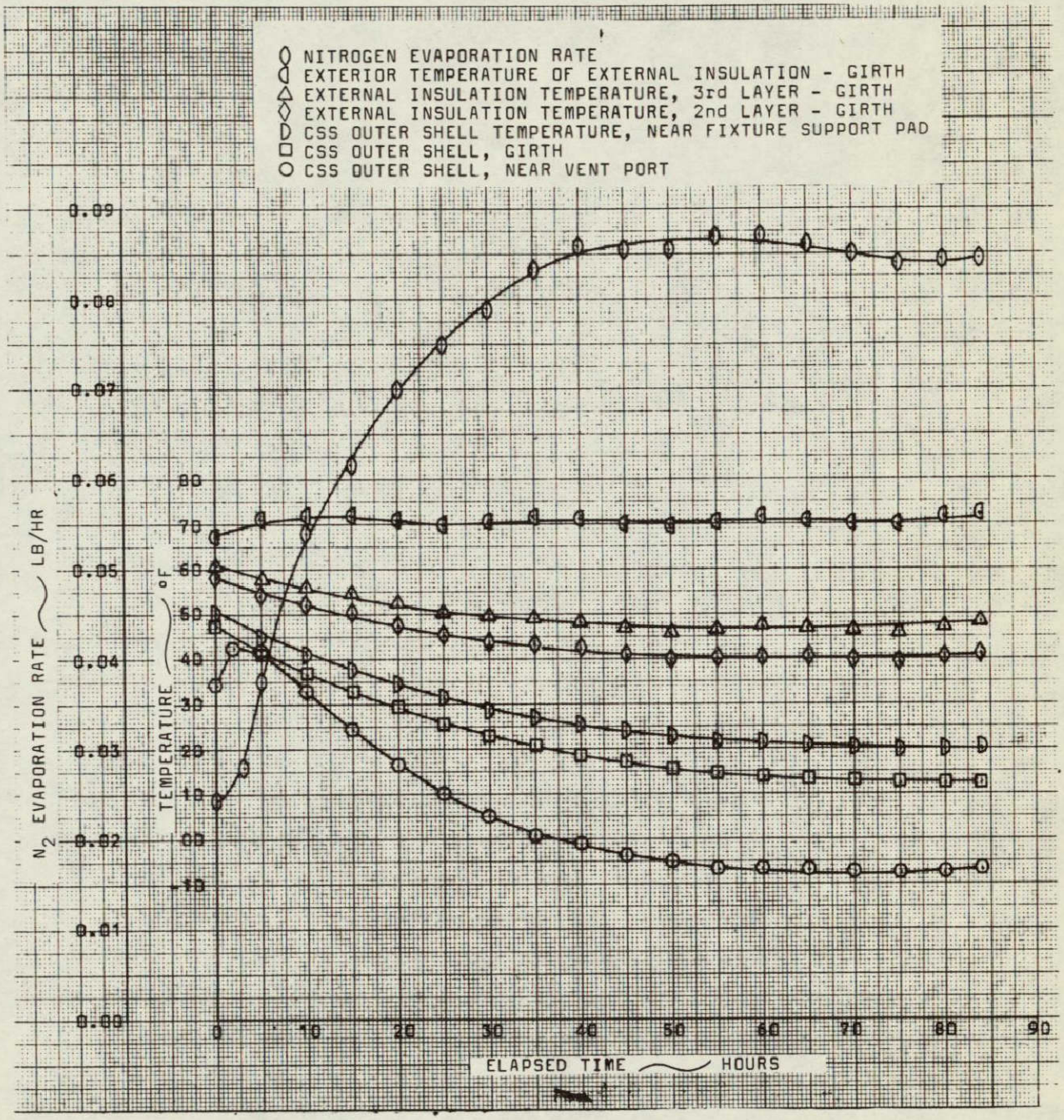

Sequence 13 CSS temperature and evaporation rate versus ET.